Master of Science Thesis in Electrical Engineering
Department of Electrical Engineering, Linköping University, 2019

Photovoltaic Power Production and Energy Storage Systems in Low-Voltage Power Grids

Jonathan Jerner and Johan Häggblom

Master of Science Thesis in Electrical Engineering

Photovoltaic Power Production and Energy Storage Systems in Low-Voltage Power Grids:

Jonathan Jerner and Johan Häggblom

LiTH-ISY-EX--19/5194--SE

Supervisor: **Daniel Jung**
ISY, Linköping University
Andreas Åkerman
Tekniska verken Linköping Nät AB

Examiner: **Christofer Sundström**
ISY, Linköping University

Division of Vehicular Systems
Department of Electrical Engineering
Linköping University
SE-581 83 Linköping, Sweden

Sammanfattning

På senare tid har det skett en ökning i antalet solcellsanläggningar som installeras i elnätet och dessa är ofta placerade i distributionsnäten nära hushållen. Eftersom distributionsnäten sällan är dimensionerade för produktion så behöver man utreda effekten av det. I det här arbetet visas det att solcellsproduktion kommer att öka spänningen i elnätet, potentiellt så mycket att de gränser elnätsägarna måste hålla nätet inom överstigs.

En modell över lågspänningsnätet skapas i MathWorks MATLAB. Modellen innehåller transformator, kablar, hushåll, energilager och solcellsanläggningar. Systemet simuleras med hjälp av en numerisk Forward Backward Sweep-lösare som beräknar effekter, strömmar och spänningar i elnätet. Solcellanläggningarna placeras ut i elnätet i olika konfigurationer tillsammans med olika konfigurationer av energilager. Resultaten från simuleringarna analyseras främst med avseende på spänningen i elnätet utifrån dess gränser.

De slutsatser som dras i arbetet är att solcellsproduktion kommer att påverka spänningen, mycket beroende på var i elnätet anläggningarna placeras och storleken hos dem. Det visas också att energilager, justering av effektfaktor hos solcellsanläggningarna eller en spänningssänkning på transformatorns lågspänningssida kan få ner spänningen i elnätet.

Abstract

In recent years, photovoltaic (PV) power production have seen an increase and the PV power systems are often located in the distribution grids close to the consumers. Since the distributions grids rarely are designed for power production, investigation of its effects is needed. It is seen in this thesis that PV power production will cause voltages to rise, potentially to levels exceeding the limits that grid owners have to abide by.

A model of a distribution grid is developed in MathWorks MATLAB. The model contains a transformer, cables, households, energy storage systems (ESS:s) and photovoltaic power systems. The system is simulated by implementing a numerical Forward Backward Sweep Method, solving for powers, currents and voltages in the grid. PV power systems are added in different configurations along with different configurations of ESS:s. The results are analysed, primarily concerning voltages and voltage limits.

It is concluded that addition of PV power production in the distribution grid affects voltages, more or less depending on where in the grid the systems are placed and what peak power they have. It is also concluded that having energy storage systems in the grid, changing the power factor of the inverter for the PV systems or lowering the transformer secondary-side voltage can bring the voltages down.

Acknowledgments

We would like to thank our examiner, Christofer Sundström (Ph.D., Assistant Professor), for inspiring us to perform our master's thesis within the field of power engineering, which was quite a new world to us, and also for providing very valuable help in the understanding of complex three-phase power calculations.

Our supervisor at the university, Daniel Jung (Ph.D., Assistant Professor), has been a very good resource for us concerning discussions in the fields of mathematics, optimisation, data presentation and organisation of the report, as well as proofreading.

Our supervisor at Tekniska verken Linköping Nät AB, Andreas Åkerman (Power Grid Development Engineer), has provided help, understanding and data regarding low-voltage distribution grids. This includes all data for the real grid, such as cables, transformer and household consumption, without which this thesis work could not have been performed and hence we are very grateful. Our thanks also go to Christian Cleber (Head of Network Development) at Tekniska verken, for allowing Andreas to use his work-time to help us.

We would also like to thank the Department of Vehicular Systems at Linköping University for inviting us to their "fika" room, for nice discussions and for providing us office space and computer equipment at the university. We specifically want to mention Max Johansson (Ph.D. student) for friendship and discussions regarding our thesis work.

Finally, we would like to thank our families and friends, including our partners Hanna and Amanda, for standing by us and supporting us through our studies.

Linköping, May 2019
Jonathan Jerner and Johan Häggblom

Contents

Notation **xi**

1 Introduction **1**
1.1 Problem Description . . . 2
1.2 Delimitations . . . 4
1.3 Approach . . . 4
1.4 Electric Power Quality . . . 5
1.5 Power Engineering Glossary . . . 6
1.6 Related Work . . . 7
1.6.1 Distribution Grid . . . 7
1.6.2 Solver Method for Distribution Grids . . . 7
1.6.3 Previous Theses . . . 8

2 Modelling **9**
2.1 Grid . . . 10
2.2 Components . . . 10
2.2.1 Cables . . . 11
2.2.2 Transformer . . . 12
2.3 Household Consumption Data . . . 15
2.4 Photovoltaic Power Production . . . 16

3 Simulation **17**
3.1 Forward Backward Sweep Method . . . 18
3.1.1 Inputs and Outputs . . . 18
3.1.2 Algorithm Overview . . . 19
3.1.3 Backward Sweep . . . 19
3.1.4 Forward Sweep . . . 21
3.1.5 Convergence . . . 22
3.2 Validation . . . 23
3.3 Real Grid . . . 26
3.4 Energy Storage Systems . . . 26

4 Analysis **29**

4.1 Evenly Distributed Power Production 30
4.2 Selectively Distributed Power Production 30
4.2.1 Greedy Search 30
4.3 Power Factor of PV Power Systems 31
4.4 Energy Storage Systems 33

5 Results **35**
5.1 Normal Case Without Production 36
5.2 PV Power Production at All Loads 38
5.3 Evenly Distributed PV Power Production 40
5.4 Selectively Distributed PV Power Production 43
5.4.1 Weak Placement 43
5.4.2 Strong Placement 45
5.5 Power Factor of PV Power Systems 47
5.6 Energy Storage Systems 49

6 Discussion **53**
6.1 Modelling 54
6.1.1 Consumption and Production Data 54
6.2 Simulation 54
6.2.1 Forward Backward Sweep Method 54
6.2.2 Validation 55
6.2.3 Energy Storage Systems 55
6.3 Results 56
6.3.1 Normal Case Without Production 56
6.3.2 PV Power Production at All Loads 56
6.3.3 Evenly Distributed PV Power Production 56
6.3.4 Selectively Distributed PV Power Production 57
6.3.5 Power Factor of PV Power Systems 58
6.3.6 Energy Storage Systems 58

7 Conclusions **61**
7.1 Future Work 62

Notation

Electric Quantities

Notation	Description	Unit	Complex Value
S	Power	VA	Yes
P	Active Power	W	No
Q	Reactive Power	VAr	No
U	Voltage	V	Yes
I	Current	A	Yes
Z	Impedance	Ω	Yes
R	Resistance	Ω	No
X	Reactance	Ω	No
Y	Admittance	S	Yes
G	Conductance	S	No
B	Susceptance	S	No

Parameters and Variables

Name	Description
U_f	Voltage, line-to-neutral
U_h	Voltage, line-to-line
I_c	Current through a connection
Z_c	Series impedance of a connection
Y_c	Shunt admittance of a connection
Z_{ser}	Series impedance matrix
Y_{shu}	Shunt admittance matrix

Abbreviations

Abbreviation	Description
AC	Alternating Current
DC	Direct Current
PV	Photovoltaic
FBSM	Forward Backward Sweep Method
ESS	Energy Storage System

Mathematical Expressions

Expression	Description
j	Imaginary unit ($j^2 = -1$)
x^*	Complex conjugate of x

1

Introduction

Increased demand for renewable electric power poses a challenge to the electric power grid. Today's power grid was designed in a society where electric power generation was concentrated to a few power plants connected to the high-voltage transmission grids. The power flow was mainly from power plants to households, from high-voltage level to low-voltage level. The renewable power sources, such as photovoltaic (PV) power systems and wind power plants, generally produce less power per site, but since they are much cheaper they can be built in much higher numbers in many more places. This means that renewable power sources often are connected to the low-voltage distribution grids, which the grids usually are not designed for [1].

In recent years, there has been a significant rise in small-scale PV power systems. Just between 2016 and 2017, the number of PV power systems installed in Östergötland, Sweden, increased from 785 to 1146 according to Table 1.1, which corresponds to a 46 % increase [2]. There are several reasons contributing to this, such as increasing environmental awareness of both companies and the general population. Saving costs on the electricity bill and generating income by selling any surplus electric power back to the grid are incentives for households and businesses.

The total electric power production in Sweden 2016 amounted to 152.5 TWh, and PV power systems contribute to about 0.09 % of this [3]. However, the rapid installation of PV power systems on the low-voltage distribution grids, designed without regards to small-scale local production of electricity, could cause problems with electric power quality [1].

As the usage of the low-voltage grid changes from being purely for distribution to a mix of distribution and production, the interest in and implementations of

	Number of Systems		Total Installed Power	
Year	2016	2017	2016	2017
Östergötland	785	1146	14.25 MW	19.83 MW
Linköping	267	372	5.36 MW	7.27 MW

Table 1.1: PV power systems in the local geographical area [2].

"smart grids" are also increasing. A smart grid is not only referring to the grid itself, but also to sensors, means of production, and other equipment used to autonomously control the use of electricity. This allows for higher usage when production is high i.e. when electricity prices are low. A potential problem with automated consumption implemented this way is that many large electrical loads might be turned on at the same time when a certain low-price threshold is reached. An example is a fleet of electric cars on standby, waiting for a low-price indicator before they begin charging. A large and rapid increase in consumption like this could affect electric power quality.

1.1 Problem Description

The system that is to be investigated is a distribution grid providing electric power to a residential area containing a 22 kV/420 V distribution transformer, cables, and 67 households. None of the households have PV power systems in reality, but such systems will be simulated along with energy storage systems. A concept sketch of the system is presented in Figure 1.1, showing three out of 67 households in the real grid (further presented in Section 3.3). At any given moment, the electric power quality must be maintained, i.e. voltage and frequency must be kept within limits and disturbances must be avoided, regardless of loads in the homes and PV power production. Historically, this has been done by electric power being continuously provided by the grid operator from large-scale power plants elsewhere. This power production has been stable, predictable and large enough for a household or a residential area on a distribution transformer to have little impact on the electric power quality in the grid [1].

A sunny summer day, it is likely that PV power production is high while electricity consumption is low. When the PV power production becomes greater than the power demand of the household where it is installed, the excess power is sold to the grid operator. In this scenario, the household goes from being a consumer to being a producer and might cause the grid voltage to increase.

Today's distribution grids are designed for high consumption and low production and not what could now be a reality - high production and low consumption [1]. The latter case might become a reality when many households, connected to the same distribution transformer, install PV power systems on their roofs. It is not fully investigated how this might affect the electric power quality and if the distribution grid can handle this load scenario. It might also vary from grid to grid.

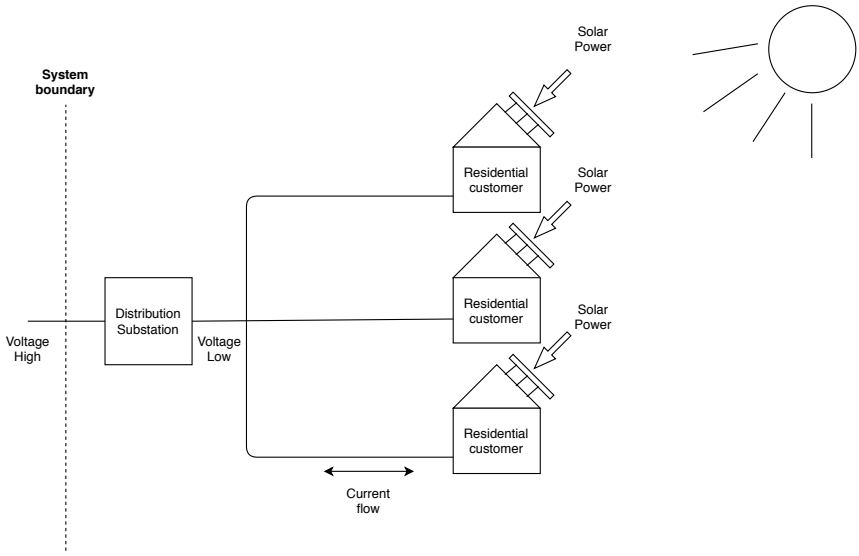

Figure 1.1: Concept sketch of the system, showing three out of 67 households in the real grid.

If the limit for PV power production is reached, considering electric power quality in the grid, a way to actively stabilise the power grid could be to use an energy storage system. This could be a battery, a hydraulic accumulator or even a flywheel and would act as a storage for any surplus electricity produced when consumption is low, to be used when conditions have changed. This approach is getting more common in, for example, Germany [1, 4].

A model of the distribution grid connecting the households is developed as well as a model of the 22 kV/420 V distribution transformer (line-to-line voltage). These are used to construct a model of the system with the main purpose being voltage analysis on the low-voltage side of the transformer [5]. The system model consists of the distribution grid, the transformer, the households, the PV power systems and the energy storage systems. This model is used for the simulation of different production and consumption scenarios.

The objective of this master thesis project is to investigate the following issues:

1. How much PV power production can a distribution grid handle before the electric power quality deteriorates?

2. How does the placement of PV power systems in the grid affect the electric power quality?

3. Can electric power quality be improved by changing the power factor of the PV power systems?

4. Can electric power quality be improved by placing energy storage systems within the grid?

1.2 Delimitations

Only radial distribution grids are considered in this thesis work. A radial grid is a grid with a hierarchical tree structure, where many loads are supplied by one power source and there is only one connection to each load bus.

The household consumption as well as the PV power production is assumed to be symmetric over the three electric phases, i.e. the power is equally large in each phase. This approach has been used in previous research such as [6]. Thus, calculations are performed for one three-phase equivalent line which also eliminates the need of a neutral line. The load power factors are assumed to be equal to one, i.e. the loads are purely resistive.

Only the low-voltage grid (420 V level) is modelled and the voltage on the high-voltage side (22 kV) of the transformer is assumed constant, see Figure 1.1. Note that these voltages are line-to-line voltages. The mains frequency is assumed to be constant at 50 Hz and waveform is not considered.

Only passive transformers with manual off-load tap changers are considered. No tap changing systems, neither manual nor automatic, and no digital power electronics are modelled.

Only underground cables over short distances are modelled. No overhead lines are considered. No temperature dependencies on electric characteristics are included.

1.3 Approach

The problem described in Section 1.1 is approached in three steps, described herein.

Modelling

Underground cables and a distribution transformer are modelled using equations from three-phase power engineering literature and electrical properties from data provided by Tekniska verken. These are combined into a model of the entire system, where the transformer model and many instances of the cable model make up a distribution grid.

Households are represented by non-controllable loads where the power consumption is specified at certain buses in the grid. Energy storage systems are modelled as controllable loads. The PV power system model used herein is developed and presented in [7] and power production is implemented as a negative load at a certain bus. Weather data for the PV power model is provided by the Swedish Meteorological and Hydrological Institute [8]. The weather data is from Norrköping, Sweden, and is assumed to be representative for a Swedish town.

Simulation

In order to simulate the system, a solver using the Forward Backward Sweep Method is developed and implemented. According to, for example, [9], this method is suitable for radial distribution grids which is what is considered in this thesis project. The implemented solver is validated using a small test system possible to calculate by hand using basic power engineering equations.

Analysis

In order to evaluate how well the grid handles PV power systems, PV power production is added in different configurations on the same timeline as the household power consumption data. The grid is simulated with the results being the basis of a voltage analysis. The analysis includes changing the power factor of the PV power production in order to evaluate how reactive power affects the voltage as well as different energy storage system configurations and their effect on the voltage. Lowering the secondary-side voltage of the transformer is also evaluated briefly.

1.4 Electric Power Quality

Electric power quality is considered according to Svensk Standard SS-EN 50160, which is the official Swedish language version of the European Standard EN 50160:2010 adopted by the Comité Européen de Normalisation Électrotechnique (CENELEC) in 2010 [10].

The SS-EN 50160 standard specifies the main properties of electric power quality for transmission and distribution grids. For this thesis work, the part regarding the low-voltage distribution grid is of special interest as it defines the voltage limits considered.

For a distribution grid, the nominal voltage U_n (line-to-neutral) is 230 V and the nominal frequency of the supply voltage is 50 Hz. For voltage, without supply interruptions, the grid should always be within ±10 % of the nominal voltage U_n. Considering this, the voltage limits are set to $U_{min} = 207\ V$ and $U_{max} = 253\ V$. Frequency changes are not considered in this work, and the frequency is therefore assumed to be static at 50 Hz.

The SS-EN 50160 standard also specifies several short-term phenomena such as voltage dips, voltage swell and flicker. Events of this short-term nature (lasting for tenths of a second) are considered to be out of scope for this thesis.

1.5 Power Engineering Glossary

A number of words and expressions used in the thesis are described herein.

AC Power Concepts

Some general power engineering concepts are presented here.

Active power Active power P (or real power) is consumed in resistive loads. The current and voltage are in phase and reverse their polarity at the same time. Their product is always larger than or equal to zero and the direction of power flow is not reversed (for a load). Active power is useful energy which can be converted into work. [11]

Reactive power Reactive power Q is consumed in inductive reactances and produced in capacitive reactances. The current and voltage are out of phase (90 degrees for a purely reactive load) and their product is thus positive for half of the cycle and negative for half of the cycle. The energy flows back and forth and there is no net transfer of energy to the load which could be converted into work. Reactive power does, however, affect voltage and current in AC components [11].

Complex power Complex power S is the complex sum of active power and reactive power, i.e. $S = P + jQ$, as indicated by the phasor S in Figure 1.2. This is useful since all practical applications utilise both active and reactive power [11].

Apparent power Apparent power $|S|$ is the product of voltage and current and also the length of the complex power phasor [11].

Power angle The power angle φ is the angle between the complex power and the active power, as indicated in Figure 1.2 [12].

Power factor The power factor $\cos\varphi$ is the ratio of the active power to the apparent power [12].

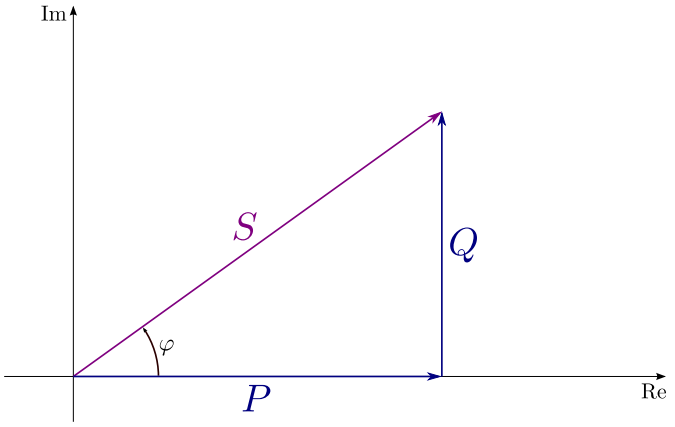

Figure 1.2: Power triangle describing complex power S, active power P, reactive power Q and power angle φ. (Eli Osherovich, CC BY-SA 3.0)

Grid Modelling Concepts

A number of grid modelling concepts specific for this thesis are presented here.

Bus A point in the network with an associated net power and voltage.

Connection A physical connection between two buses in which current can flow, such as a cable or a transformer. The start bus of a connection is the end closer to the transformer and the end bus is the end farther from the transformer.

Child Connection A is a child to connection B if its start bus is the end bus of connection B. Bus A is a child to bus B if the connection which has its end bus in bus A has its start bus in bus B.

Parent Connection A is a parent to connection B if its end bus is the start bus of connection B. Bus A is a parent to bus B if a connection which has its start bus in bus A has its end bus in bus B.

1.6 Related Work

A selection of the related work the authors have considered during the thesis project is presented here.

1.6.1 Distribution Grid

In [13], a real distribution grid is simulated as a three-phase system with PV power production using commercial simulation software. In the article, voltage unbalance problems are studied and the authors try to solve them by implementing energy storage systems.

The same authors as in [13] also wrote another article, [4] where control strategies for energy storage systems for PV power production are examined, with the goal being to avoid voltage transients in the distribution grid caused by PV power production. This article focus on the implementation of an energy storage system and the control strategies. It also touches on the subject of PV power systems producing reactive power, which this thesis also includes in the analysis.

1.6.2 Solver Method for Distribution Grids

In [14], several methods for radial distribution grid calculations are examined and discussed. The article discusses advantages and disadvantages concerning convergence, sensitivity, accuracy and more. The article concludes that the Forward Backward Sweep Method (FBSM) is a very robust and numerically efficient method.

The FBSM method is implemented in [15] and compared to the Fast Decoupled Load Flow method (FDLF) as well as the Newton-Rhapson method. When testing the methods, IEEE Test Feeders (9 and 33) were used and FBSM was found to be the most efficient.

In [16], a version of an FBSM method is implemented for a three-phase system. The method used in this article tries to split the real and complex parts of each electrical quantity into two independent systems in the forward sweep. The results are compared against a more classical approach to the FBSM method and are found to produce similar results but slightly faster in terms of the number of iterations and the computational time required.

1.6.3 Previous Theses

Some previously written master theses with similar approach and methodology as this thesis project are [17–19]. The main difference between those theses and this thesis is their use of commercial simulation software to simulate the distribution grid, compared to implementing self-made models and a self-made solver as well as performing a different set of analyses.

In [18, 19], PV power systems and energy storage systems are considered but mostly in the aspect of profitability. This thesis instead focuses on voltage analysis within the grid. The collected data is transformed into power curves with a mean value per day, while in this thesis, the sample time is kept hourly.

In [17], PV power systems' influence on the distribution grid is the main consideration. However, a simpler PV power system model is used and the household consumption data is based on yearly consumption converted into a power curve. In [17], the analysis is performed partly by placing solar panels evenly in the grid similar to what is done in this thesis, but a worse-case placement is not considered.

2
Modelling

In this thesis work, the issues are investigated by developing a simulation model of system (see Figure 1.1) and simulating different load scenarios where the PV power production is expected to vary substantially. To develop and validate the intended models, the following is supplied by external parties:

Data from households used to model the electric power consumption is supplied by the local electric power grid operator, Tekniska verken Linköping Nät AB or Tekniska verken in short. Specifications for the low-voltage grid, concerning distribution transformer, cables, etc. is also supplied by Tekniska verken and is used to model the cables and the transformer. Requirements on electric power quality is considered according to Swedish Standard SS-EN 50160, further explained in Section 1.4.

A previously developed model of photovoltaic cell systems is supplied by Linköping University, created during previous thesis project [7]. This model together with weather data supplied by the Swedish Meteorological and Hydrological Institute [8] is used in the PV power production model.

The main objective for the models is to model a system where voltage transients, mainly on the low voltage side of the transformer and at load buses, can be studied. For each component, models of various complexity are studied and chosen based on the needs for the complete system to be accurate.

2.1 Grid

The complete system consists of one transformer and cables connected in various ways, reaching each load bus. How each bus is connected to the rest of the grid, and what kind of connection that is, is given in data provided by Tekniska verken and is used to create the complete system model. For each connection in the input data, the start bus and end bus are stored along with the cable name and length. The name of the connection is then matched against a database whose content structure is shown in Table 2.1, containing all of the possible cable types. When a match is found, the electrical quantities are calculated based on the length of the cable and stored in the matrices $Z_{ser} \in \mathbb{C}^{n\times n}$ for series impedance and $Y_{shu} \in \mathbb{C}^{n\times n}$ for shunt admittance. Here, n is the number of buses in the system and each value represents the series impedance and shunt admittance between the start bus and the end bus, respectively. This approach is based on the methods used in [20–22]. In Figure 2.1, a real grid is shown, whose data is provided by Tekniska verken.

Parameter	Abbrev.	Unit	Description
Name	-	-	Name of the cable
Area	A	mm^2	Cross section area
Material	-	-	Material of conductor
Type	-	-	Underground or overhead
Resistance	R	Ω/km	Resistance per km
Reactance	X	Ω/km	Reactance per km
Susceptance	Bd	$\mu S/km$	Susceptance per km
Max current	I	A	Maximum current allowed

Table 2.1: The content structure of the cable database.

The red buses are loads which are given a unique reference number when added to the system and the connection between the top buses (bus one and bus two) is the transformer. The remaining buses are different cables being joined together creating the complete grid.

2.2 Components

In this section, the implemented models are presented. All models are implemented in MathWorks MATLAB and the main system model consists of a transformer, underground cables and loads (households). For the analysis, these are combined with models of PV power systems and energy storage systems. All models are static, i.e. they do not contain any time derivatives. Components such as cables and transformers contain dynamics in reality but the choice to use only static models is considered reasonable within the scope of this thesis. For example, the time constants for the real component dynamics will be in the scale of milliseconds, according to [23], and the consumption data and PV power production data used has a sample time of one hour. The calculations for one time

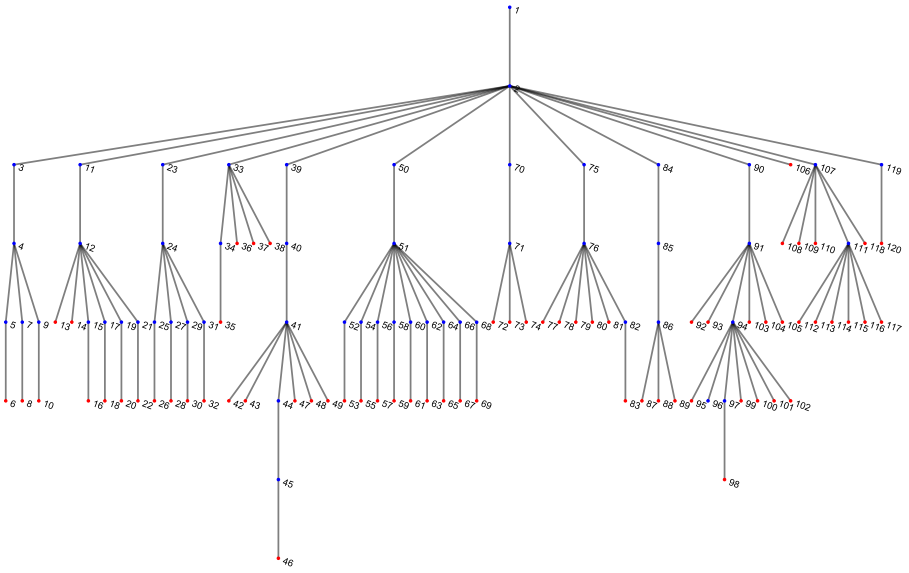

Figure 2.1: Grid plot of the real grid, Hallonvägen, showing all connections in black, load buses in red and other buses in blue. The transformer is located between bus one and bus two.

step does not at all affect the computations at another time step, except when an energy storage system is used and the battery state of charge is carried over from one time step to the next. For further details, see Section 3.4.

2.2.1 Cables

Cables in the model can have current flowing through them in either direction as described by

$$I_c = \frac{S}{\sqrt{3}U_h}. \tag{2.1}$$

Cables cause a power loss,

$$S_{loss} = 3Z_c|I_c^2| = 3Z_c I_c I_c^* \tag{2.2}$$

and therefore also cause a voltage drop across their length,

$$U_\Delta = -\sqrt{3}I_c Z_c, \tag{2.3}$$

regardless of current direction.

An equivalent Π model is chosen for the cable model as it is commonly used in power system modelling [20, 21, 23]. The model consists of series impedance, Z_c and shunt capacitance, Y_c, see Figure 2.2. For cables shorter than approximately 80 km, the shunt capacitance can be modelled as zero [20].

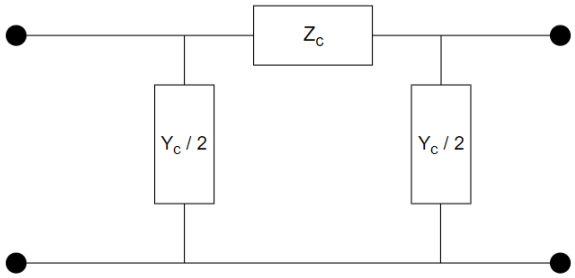

Figure 2.2: The implemented cable model, an equivalent Π circuit.

2.2.2 Transformer

The main function of a transformer is to increase or decrease the voltage between two or more circuits. In this system the two circuits are the 22 kV transmission grid on the high voltage side and the 420 V distribution grid on the low voltage side. Note that these voltages are line-to-line voltages.

A transformer uses two or more coupled windings on a magnetic core to transfer electrical energy. Simply put, when the current passes through the primary coil, a magnetic field is created around the core which in turn induces a current through the secondary coil. However, there are also losses to consider when modelling a non-ideal transformer.

The losses considered in this model are based on the two most commonly considered when modelling a practical transformer, idling losses and load losses. Idling losses are also called core losses or magnetising losses and occur in the core whenever the transformer is energised. The load losses are also called copper losses or short-circuit losses and occur as a result of the current flowing through the copper windings. The losses are implemented in the transformer model as the impedances Z_0 for idling losses and Z_{2k} for load losses as shown in Figure 2.3 [20, 23, 24].

Per-Unit System

It is common during power system analysis to use a per-unit system. This refers to a normalisation where quantities are expressed as fractions of a defined base unit quantity instead of using physical units. Base values are commonly but not necessarily chosen as the power and voltage ratings of the transformer, in order to have principal variables equal to one under rated conditions. Some base values can be chosen independently while others will follow based on fundamental relationships between system variables [20]. When choosing quantities in this manner, any other electrical quantity can be defined in per-unit as well. The purpose of this is to be able to do calculations on the circuit as if all components of

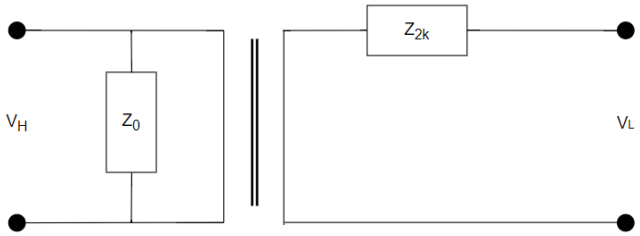

Figure 2.3: Transformer model based on given data.

the circuit would be at the same voltage level and it can also minimise computational effort [20]. Example 2.1 helps to explain why this is used.

Example 2.1

Given the transformer in Figure 2.4 with the ratings from Table 2.2 and assuming a current of $I_1 = 28.86\,\text{A}$ on the primary side, the current I_2 can be calculated as 721.68 A on the secondary side.

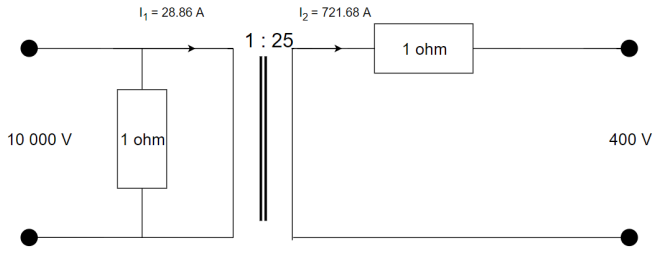

Figure 2.4: Example transformer.

Given that the transformer is rated at $S = 500\,\text{kVA}$, $U_1 = 10\,\text{kV}$ and $U_2 = 400\,\text{V}$, these values can be selected as per-unit base values. The current and impedance base values can now be calculated using

$$I_{base} = \frac{S}{\sqrt{3}U_{base}} \tag{2.4}$$

and

$$Z_{base} = \frac{U_{base}}{\sqrt{3}I_{base}} = \frac{U_{base}^2}{S}. \tag{2.5}$$

Quantity	Value
S	500 000 VA
U_1	10 000 V
U_2	400 V
Z_{2k}	1 Ω
Z_0	1 Ω

Table 2.2: Transformer ratings.

Per-Unit Base	Value
S_{base}	500 000 VA
U_{base1}	10 000 V
U_{base2}	400 V
I_{base1}	28.86 A
I_{base2}	721.68 A
Z_{base1}	200 Ω
Z_{base2}	0.32 Ω

Table 2.3: Per-unit base values.

Calculated per-unit base values are presented in Table 2.3 and the transformer model can then be rewritten in per-unit values as shown in Figure 2.5, and then be simplified to the circuit shown in Figure 2.6.

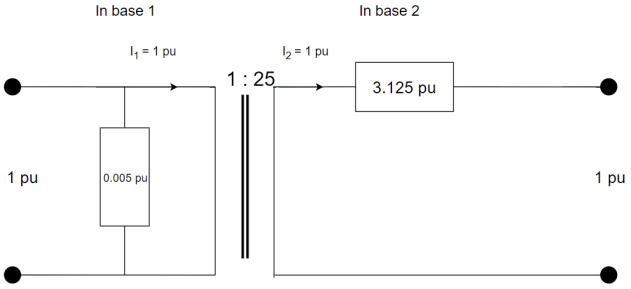

Figure 2.5: Example transformer in per-unit.

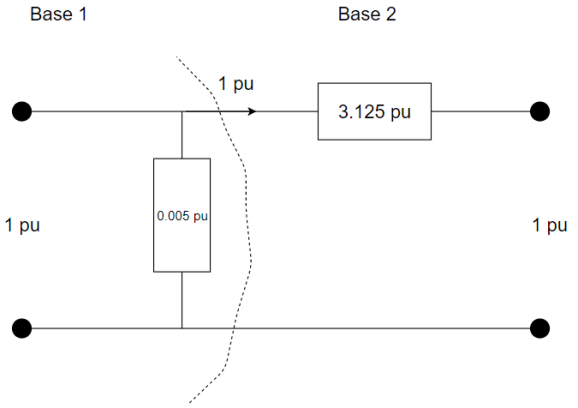

Figure 2.6: Example transformer simplified.

As can be seen in Example 2.1, the model can be reduced to a circuit very similar to the equivalent Π model implemented for cables. By inverting Z_0 and splitting it into two parts as well as placing the halves on each side of the series impedance, the equivalent Π model, Figure 2.7, can be used for the transformer as well [23, 24] . This means that the same equations as for cables, Equations (2.1) to (2.3), can be used for the transformer.

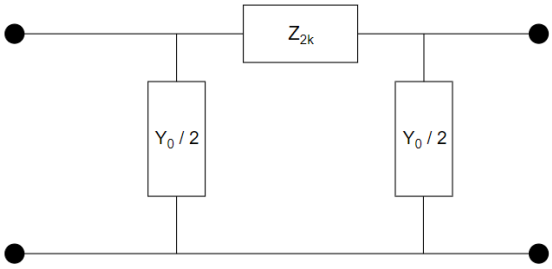

Figure 2.7: Implemented transformer model.

2.3 Household Consumption Data

For each load (bottom of the bus tree, Figure 2.1) power consumption is needed for the solver to be able to calculate the power throughout the system. The power consumption data is provided by Tekniska verken and comes in the form of text files with reference numbers. These reference numbers are matched against the reference numbers of the load buses in the grid so that they get the correct consumption data.

The data is provided as integer values accumulated until 1 kWh active power is reached and stored for every hour of a year. For the sake of simplicity and not knowing how the data points marked as zero accumulates to one, any zero value is treated as zero consumption and a following one value is treated as 1 kWh consumption for that sample. In Figure 2.8, data for four load buses can be seen over a two-week period. It should be noted that more realistic consumption data would include reactive power. This has not been measured in this data set.

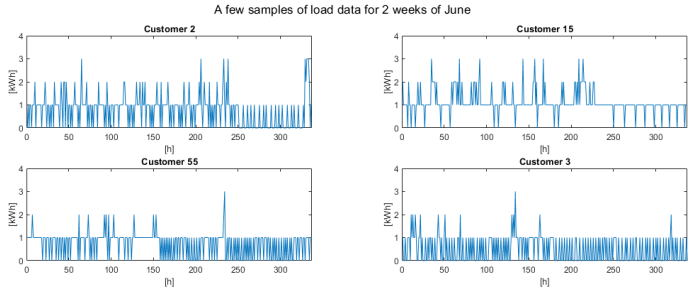

Figure 2.8: Samples of load data provided by Tekniska verken.

2.4 Photovoltaic Power Production

A previously developed photovoltaic power model is taken from [7]. The model outputs power production values using static equations with inputs of solar irradiance, orientation and tilt of the solar panel. Solar irradiance data is provided by the Swedish Meteorological and Hydrological Institute, SMHI, for the nearest location. To gain the highest possible output, the solar panels are assumed to be installed facing south. Tilt refers to the inclination angle of the panel and the output varies little with tilt so a tilt angle of 22 degrees is assumed for the sake of simplicity [7].

To simulate PV power production, the solar data from 2015 is used as it has already been processed when the model was created. The data is limited to hourly values, and therefore the production is regarded the same for all solar panels in the complete systems at any given time. Examples of the PV power production added to the grid can be seen in Figure 2.9, where it can be noted that the power is much higher in summer than in winter or fall.

The model output is approximately 8 kW (peak), making it a reasonable system to consider for the average household [25]. Hereafter, the described settings for the PV power system model are referred to as the default PV power system.

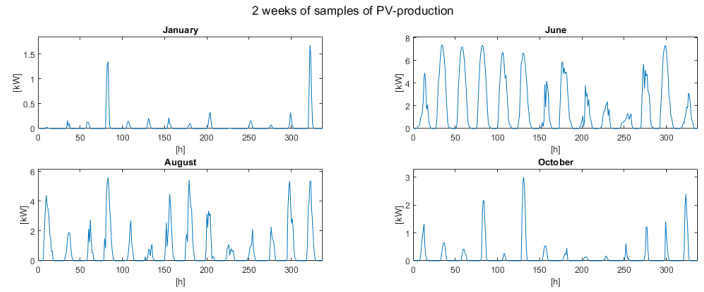

Figure 2.9: Samples of PV power production data over two weeks during four different months.

3
Simulation

In this chapter the implemented solver method is described and a small test system is used for validation. The real grid used for the analysis as well as the implementation of an energy storage system is also introduced.

The Forward Backward Sweep Method (FBSM) is described in depth, since it is considered to be a central part of this thesis work. The overall method is described using an algorithm, and the solver function's inputs and outputs, the forward and backward sweeps including their equations and the convergence criteria are described.

The FBSM solver is validated by designing a small test system possible to calculate by hand. It is first calculated using the solver function and then verified by hand. The convergence of the FBSM algorithm is demonstrated for this small test system.

The real grid used in the analysis is presented considering location, size and transformer specifications. The algorithm of the energy storage system implementation and the specifications of the different versions of it are also presented herein.

3.1 Forward Backward Sweep Method

The solver function uses the FBSM method, which is an iterative method used to find voltages, powers and currents in all buses in the grid. This is done from given grid data, fixed slack bus voltage, initial voltage estimates at all other buses and power demands at each load bus. The implementation is based on the method described in [9].

Forwards is defined as the direction towards the load buses and backwards as the direction towards the transformer bus. This is similar to the power definition where positive power indicates net power consumption at a bus (power flow towards the bus) and negative power indicates net power production.

3.1.1 Inputs and Outputs

The solver has one output (the $Results$ structure) and ten inputs, of which five are mandatory (Z_{ser}, Y_{shu}, S_{in}, U_{in} and Ξ).

$Z_{ser} \in \mathbb{C}^{n \times n}$ is the series impedance matrix where n is the number of buses in the system. It contains the series impedance for all connections (between two buses), i.e. the cable and transformer impedances, where $Z_{ser}(start, end) = value$. The value is a complex number $Z = R + jX$ where R is the connection resistance and X is the connection reactance. It is theoretically possible to define different impedances in different directions, but since this is not reasonable in practice, Z_{ser} will always be symmetric.

$Y_{shu} \in \mathbb{C}^{n \times n}$ contains the shunt admittances for all connections. The matrix elements contains complex numbers on the form $Y = G + jB$ where G is the shunt conductance and B is the shunt susceptance. The implementation is made in such a way that a positive value for the conductance will create a positive active power (consumption or loss in the connection) and a positive value for the susceptance will create a negative reactive power (production or generation in the connection). The shunt conductance is generally regarded as zero and the shunt susceptance is also small compared to the series impedance for short cables ($l \lessapprox 80$km) [20]. If shunt admittance is not used, all values are set to zero.

$S_{in} \in \mathbb{C}^{n \times 1}$ contains the net powers (demand or production) for all load buses. The values are set as complex numbers on the form $S = P + jQ$ for each load bus, where P is active power and Q is reactive power, and to zero for all other buses. The powers for non-load buses are to be calculated.

$U_{in} \in \mathbb{C}^{n \times 1}$ is a vector whose first element is the fixed voltage (magnitude and angle) in the slack bus (bus 1) which thus is the angular reference for the other buses. The angle for the slack bus is normally set to zero. The rest of the elements are the initial voltage estimates in the other buses, which may have (but must not have) an estimated initial angle specified. All voltage values are set in complex (rectangular) form.

$\Xi \in \mathbb{N}^{(n-1) \times 2}$ contains the bus numbers (start bus and end bus) for each connection between two buses. Each connection is represented by a row and the first

column contains the start buses whilst the second column contains the end buses. Parallel connections between the same buses are not supported.

The *Results* output structure contains the fields described in Table 3.1. All electrical quantities are the values from the last iteration.

Table 3.1: Fields in the *Results* output structure of the FBSM solver.

Results field	Description
S_{out}	Power calculation (per bus)
S_{loss}	Power loss calculation (per connection)
U_{out}	Voltage calculation (per bus)
U_{delta}	Voltage loss calculation (per connection)
I_{out}	Current calculation (per connection)
n_{iters}	Number of iterations

3.1.2 Algorithm Overview

The overall iterative method can be described using the pseudo-code in Algorithm 1. The forward and backward sweeps are described in more detail in Sections 3.1.3 and 3.1.4, respectively, and the convergence criteria in Section 3.1.5.

3.1.3 Backward Sweep

The iterative method begins with a backward sweep starting the calculations from the load bus ends and proceeding connection by connection through the grid, including the transformer, all the way to the slack bus. It is very important to ensure that all connections are calculated in the correct order to get a correct result. It is necessary that the calculations for all of a connection's children in the grid are already done before the calculations for the current connection can be started. The backward sweep loops through all connections defined in the Ξ matrix. In each step, the solver uses this matrix to check if any children to the current connection exist in the grid. If there are any, all those connections must be marked as done in order for the current connection to get a clearance for calculation. If no clearance is given, the solver skips this connection and continues with the next. The process described herein is repeated until all connections are marked as calculated. This makes the solver independent of in which order the connections are defined, and if placed in the best possible order, the outer loop will only need to run once. The order will only affect the calculation time.

For each connection in the grid, the backward sweep begins by calculating the current through the connection. If the connection is a connection to a load bus, i.e. it does not have any children, the current is found using the net power at the end bus and the voltage from the previous iteration (since it is yet to be calculated for this iteration) as

$$I_{conn,i} = \left(\frac{S_{end,i}}{\sqrt{3} U_{end,i-1}} \right)^* \tag{3.1}$$

```
load net power at load buses;
load fixed slack bus voltage;
load voltage estimates;
while not convergence do
    while not all connections calculated do          // Backward sweep
        foreach connection do
            find start bus and end bus;
            if no non-calculated children then
                calculate connection current;
                calculate connection losses;
                calculate connection power;
                calculate start bus power;
            else
                skip to next connection;
            end
        end
    end
    while not all connections calculated do           // Forward sweep
        foreach connection do
            find start bus and end bus;
            if no non-calculated parents then
                calculate voltage drop over connection;
                calculate voltage at end bus;
            else
                skip to next connection;
            end
        end
    end
end
```

Algorithm 1: Pseudo-code describing the Forward Backward Sweep Method algorithm.

where index i denotes the current iteration, $i-1$ the previous iteration, etc.

If the connection is a connection to one or more children, the current is the sum of the currents in the children, i.e.

$$I_{conn,i} = \sum_{children} I_{child,i}. \tag{3.2}$$

The power losses over a connection, both active and reactive, are found using the current and the series impedance of the connection, as

$$S_{loss,i} = 3I_{conn,i}I^*_{conn,i}Z_{ser}. \tag{3.3}$$

Note that for a capacitive connection, i.e. with a negative imaginary part of Z_{ser}, the connection might generate reactive power.

The total power flow through the connection is the power required at the end bus plus the power losses, i.e.

$$S_{conn,i} = S_{end,i} + S_{loss,i}. \tag{3.4}$$

The power at the start bus of the connection is added to the power already calculated for this bus,

$$S_{start,i} := S_{start,i} + S_{conn,i}, \tag{3.5}$$

to get the correct total power in a joint with many connections. The current connection is then marked as done and the above calculations in the backward sweep are made for all connections, according to the FBSM method described in Algorithm 1.

3.1.4 Forward Sweep

The forward sweep begins the calculations from the slack bus and proceeds connection by connection through the grid, including the transformer, all the way to every load bus. In the same way as for the backward sweep, it is necessary that the calculations are made in the correct order. In this case, this means that the calculations of all of a connection's parents in the grid must already be done before the calculations for the current connection can be started. The forward sweep also loops through all connections defined in the Ξ matrix. In each step, the solver uses this matrix to check if any parents to the current connection exist in the grid. If there are any, all those connections must be marked as done in order for the current connection to get a clearance for calculation. If no clearance is given, the solver skips this connection and continues with the next. The process described herein is repeated until all connections are marked as calculated. This has the same advantages as described for the backward sweep.

For each connection in the grid, the forward sweep begins by calculating the voltage difference over the connection. This is done using the current calculated in the backward sweep and the connection's series impedance, as

$$\Delta U_i = -\sqrt{3}I_{conn,i}Z_{ser} \tag{3.6}$$

The sign is negative since a positive current (power flow to the loads) causes a voltage loss.

The voltage at the connection's end bus is then calculated using the voltage at the start bus and the voltage difference, as

$$U_{end,i} = U_{start,i} + \Delta U_i. \tag{3.7}$$

The current connection is then marked as done and the above calculations in the forward sweep are made for all connections, according to the FBSM method described in Algorithm 1.

3.1.5 Convergence

The steps described above are performed twice using an outer loop before the solver checks if the convergence criteria are met. This corresponds to the third iteration since the first iteration will contain input values and estimates only and the second iteration is thus when the first calculations are performed.

Convergence is assumed when both the power criterion

$$\max \left| S_{bus,i} - S_{bus,i-1} \right| < \varepsilon \tag{3.8}$$

and the voltage criterion

$$\max \left| U_{bus,i} - U_{bus,i-1} \right| < \varepsilon \tag{3.9}$$

are fulfilled for all buses, and the current criterion

$$\max \left| I_{conn,i} - I_{conn,i-1} \right| < \varepsilon \tag{3.10}$$

is fulfilled for all connections. The convergence limit ε is set to 10^{-4} unless anything else is specified in a certain context.

3.2 Validation

In order to validate the calculations made by the FBSM solver, a small test system possible to calculate by hand was designed and implemented. It is very simple and consists of four buses of which one is a slack bus and two are loads, and three connections between the buses forming a Y-shape. The test system is depicted in Figure 3.1.

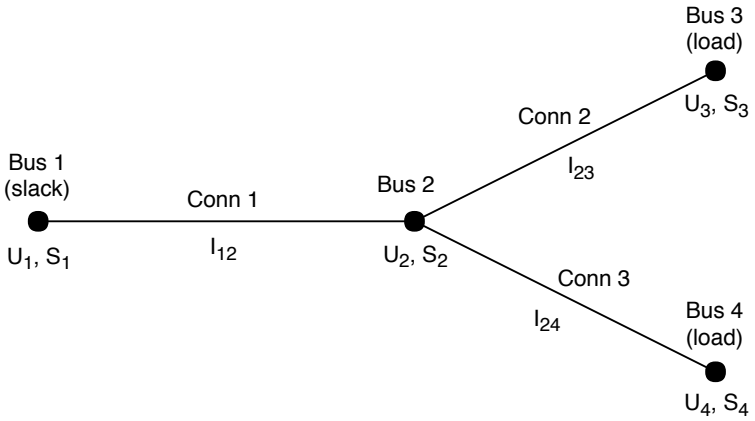

Figure 3.1: Test system with four buses, three connections and two loads.

All connections are cables with series impedance $Z = 1 + \mathrm{j}0.1$, i.e. with a resistance of $1\,\Omega$ and a reactance of $0.1\,\Omega$ (inductive). Nu shunt capacitance is considered. The fixed voltage at the slack bus (bus 1) is set to $U_1 = 400 + \mathrm{j}0$, i.e. a voltage magnitude of 400 V with an angle of zero. This is the angular reference for all other buses. The non-slack buses are initialised with a voltage magnitude estimate of 400 V. Note that these are line-to-line voltages.

The complex load specified for bus 3 is $S_3 = 3000 + \mathrm{j}2250$, i.e. an inductive load with power factor $\cos\phi = 0.8$ consuming 3000 W active power (P) and 2250 VAr reactive power (Q). The complex load specified for bus 4 is $S_4 = 2000 - \mathrm{j}1500$, i.e. a capacitive load with power factor $\cos\phi = 0.8$ consuming 2000 W active power (P) and generating 1500 VAr reactive power (Q).

The solver will find the voltage magnitudes and angles for the non-slack buses, the net power requirements (both active and reactive) for the non-load buses and the currents and losses in each connection.

The results being output by the solver when evaluating the test system are shown in Tables 3.2 and 3.3.

The results from the FBSM solver are verified using the following hand calculations. The voltage in the slack bus is set to the known value of 400 V, the currents in the connections are set to the values found using the FBSM solver and the cable

Bus	Power (1×10^3 VA)	Voltage (1×10^2 V)
1	5.3222 + j0.7822	4.0000 + j0.0000
2	5.1414 + j0.7641	3.8650 + j0.0062
3	3.0000 + j2.2500	3.7789 + j0.0566
4	2.0000 − j1.5000	3.8161 − j0.0378

Table 3.2: Power and voltage results for each bus in the test system found using the FBSM solver.

Connection	Current (A)	Power loss (1×10^2 VA)
1	7.6820 − j1.1290	1.8086 + j0.1809
2	4.6339 − j3.3683	0.9845 + j0.0985
3	3.0481 + j2.2392	0.4291 + j0.0429

Table 3.3: Current and power loss results for each connection in the test system, found using the FBSM solver.

impedances are set the same as before,

$$U_1 = 400 + 0j \tag{3.11}$$
$$I_{12} = 7.6820 - 1.1290j \tag{3.12}$$
$$I_{23} = 4.6339 - 3.3683j \tag{3.13}$$
$$I_{24} = 3.0481 + 2.2392j \tag{3.14}$$
$$Z_i = 1 + 0.1j \quad i \in [1, 3] \tag{3.15}$$

The voltage difference over each connection is calculated using the connection's current and impedance, according to

$$U_{\Delta 12} = \sqrt{3} Z_1 I_{12} = -13.5012 + 0.6249j \tag{3.16}$$
$$U_{\Delta 23} = \sqrt{3} Z_2 I_{23} = -8.6096 + 5.0315j \tag{3.17}$$
$$U_{\Delta 24} = \sqrt{3} Z_3 I_{24} = -4.8916 - 4.4064j. \tag{3.18}$$

The bus voltages are then calculated using the slack bus voltage and the voltage difference in each connection according to

$$U_2 = U_1 + U_{\Delta 12} = (3.8650 + 0.0062j) \times 10^2 \tag{3.19}$$
$$U_3 = U_2 + U_{\Delta 23} = (3.7789 + 0.0566j) \times 10^2 \tag{3.20}$$
$$U_4 = U_2 + U_{\Delta 24} = (3.8161 - 0.0378j) \times 10^2. \tag{3.21}$$

The net power in each bus is found using the voltage and the current, according

to

$$S_1 = \sqrt{3}U_1 I_{12}^* = (5.3222 + 0.7822j) \times 10^3 \tag{3.22}$$

$$S_2 = \sqrt{3}U_2 I_{12}^* = (5.1414 + 0.7641j) \times 10^3 \tag{3.23}$$

$$S_3 = \sqrt{3}U_3 I_{23}^* = (3.0000 + 2.2500j) \times 10^3 \tag{3.24}$$

$$S_4 = \sqrt{3}U_4 I_{24}^* = (2.0000 - 1.5000j) \times 10^3. \tag{3.25}$$

The results from the hand calculations match those from the FBSM solver. The convergence of the voltage and power calculations for the test system is shown in Figure 3.2.

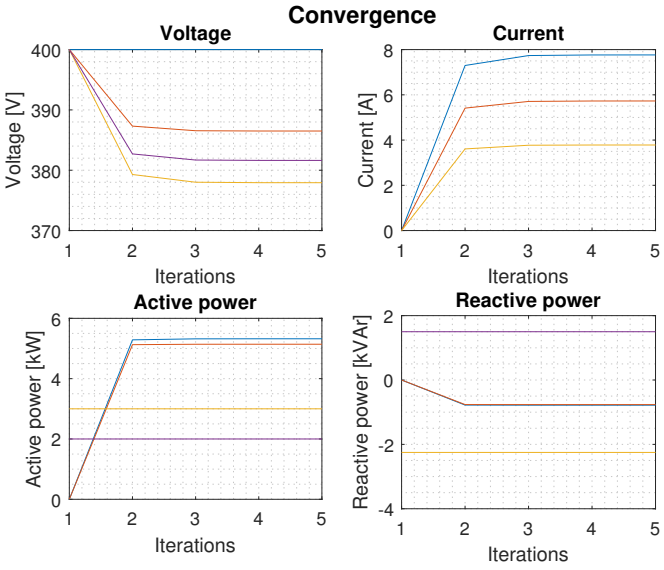

Figure 3.2: Convergence of the FBSM algorithm for voltages, currents and powers in the test system.

3.3 Real Grid

The real distribution grid whose data is provided by Tekniska verken is used for all analysis presented in this report. It is called Hallonvägen and is physically located in Katrineholm, Sweden. A tree grid plot of Hallonvägen is presented in Figure 2.1. The grid consists of 118 cables (connections) with different lengths and specifications and 119 buses. The cables generally have a conductor area of 240 mm^2 in the main branches and a conductor area of 10 mm^2 closer to the households. In the computations, a special non-physical transformer connection is added, making it 119 connections and 120 buses in total. The transformer is of the Strömberg brand and its data can be seen in Table 3.4. The transformer secondary-side voltage U_2 is set to 420 V (line-to-line). This means that the line-to-neutral voltage U_f is 242 V, already 12 V higher than the nominal value of 230 V. Index 1 denotes primary-side and index 2 denotes secondary-side values. Impedance values are given as a percentage of the rated values.

Quantity	Value
$\|S\|_{max}$	500 kVA
U_1	22 000 V
U_2	420 V
Z_{2k}	4.78 %
Z_0	0 %

Table 3.4: Transformer data for the real grid T085 Hallonvägen. Index 1 denotes primary-side and index 2 denotes secondary-side values. Impedance values are given as a percentage of the rated values.

3.4 Energy Storage Systems

Two versions of energy storage systems (ESS:s) are implemented in order to evaluate whether they can help keeping the voltage at the load buses within the limits when the PV power production is high. The first version consists of one large ESS placed at bus 120 (near the transformer) and the second version has one small ESS at each load bus, making it 67 energy storage systems in total. The first one represents a centralised ESS and the second one if each household has an ESS. Their specifications are described in Table 3.5. The charging powers of the two ESS versions are deliberately chosen in order to achieve the same total power for 67 small ESS:s as for one large ESS. Capacity is arbitrary since the power from discharge of the ESS:s is not put back onto the grid.

The implementation is made in such a way that the script stepping through the timeline in each time step first runs the solver to check how the voltages in all grid buses would have become with no energy storage system enabled. If the voltage at a bus where an energy storage is situated would have reached a certain threshold, here set to 245 V (line-to-neutral), the energy storage at that bus will

	Charging power	Capacity	At buses
Small	1 kW	20 kWh	All loads
Large	67 kW	500 kWh	Bus 120 only

Table 3.5: Specifications for the two different versions of energy storage systems.

start charging. The charging power will be the default charging power from Table 3.5 unless that power would lead to an overcharge. Then the charging power is adjusted to make sure that the charging stops when the storage is full. When the state of charge has reached 100 %, it is reset to zero. This could, for example, represent an electric vehicle being charged and the energy being used elsewhere. Thus, no discharge is considered and an energy storage system only increases the power consumption at its bus at certain times. The control strategy for charging, charge reset and voltage calculations when using one or more energy storage systems is described in Algorithm 2.

```
foreach time step do
    calculate voltages (storage disabled);
    foreach energy storage system do
        if storage full then
            reset state of charge;
        else
            state of charge as in previous time step;
        end
        if voltage threshold reached then
            if will not overcharge then
                charge with default power;
                increase state of charge;
                adjust power at bus;
            else
                charge with lowered power;
                increase state of charge;
                adjust power at bus;
            end
        else
            do not charge;
        end
        calculate voltages (storage enabled);
    end
    save results;
end
```

Algorithm 2: The control strategy for charging, charge reset and voltage calculations when using one or more energy storage systems.

4

Analysis

The purpose of the conducted analyses is to examine the grid voltages during different cases of PV power production at the load buses, i.e. the robustness of the grid. One way to implement the PV power production in the grid is to distribute the PV power evenly across all loads. A problem with this approach is that it is not a very probable scenario at the time of writing. If more households opt to install PV power systems, it could, however, be a probable scenario in the future. As of now, it is likely that only some of the households have PV power systems installed and since the two scenarios are expected to affect voltages differently, both scenarios are investigated.

For robustness, it is relevant to investigate the minimum number of households with PV power systems it takes to topple the electric power quality. When applying the principle of selected load buses having PV power production, the problem is how to select which loads to analyse. For the real grid, Hallonvägen, which has 67 possible loads to choose from, just selecting as few as ten loads has 2.5×10^{11} possible combinations. Such an exhaustive search is simply not feasible.

To find the order in which the PV power systems should be added to get a worst-case or a best-case scenario, a greedy search algorithm is implemented. The results from this algorithm will either be the weakest or the strongest placement order, i.e. the placement order that handles the least amount of PV power systems or the order that handles the most amount of PV power systems, concerning voltage limits, depending on which objective function is chosen.

Finally, the effects of changing the power factor of the PV power production, adding energy storage systems to the grid and changing the secondary-side voltage of the transformer are also investigated, since these methods are known to affect voltages in the grid.

4.1 Evenly Distributed Power Production

Evenly distributed power production refers to production being added at all load buses in the grid. The analysis is conducted by starting with a very low PV power production at each household and gradually increasing it until a voltage limit is reached somewhere in the grid. The purpose of this analysis is to determine the maximum size of the PV power systems installed in the grid if all households were to install a system each, as well as finding the maximum total power production in the grid.

4.2 Selectively Distributed Power Production

In the case of selectively distributed power production, a full default PV power system is added to selected loads. The analysis is conducted by starting with one load being given PV power production and then gradually adding more until a voltage limit is reached. The placement is decided by the results of a previously run greedy search of the real system (Hallonvägen), further explained in Section 4.2.1.

The purpose of this analysis is to evaluate the robustness of the grid when PV power systems are installed at a subset of the households. The systems will be added in the weakest order and the strongest order to find the lower limit and the upper limit, respectively, of when problems with electric power quality potentially can occur.

4.2.1 Greedy Search

A greedy search algorithm is used to assess the "strength" of the load buses in the grid. It is implemented to find the weakest and the strongest placement order, i.e. the placement order that handles the least amount of PV power systems and the placement order that handles the highest amount of PV power systems.

Greedy search is a heuristic optimisation algorithm. In short, the algorithm looks at a set of choices at a given point and optimises for that step before looking at the next set of choices until a final sequence is reached. Due to the nature of this algorithm and the scale of the grid, it is hard to guarantee that the global optimum is found, but a optimisation problem of this scale is deemed out of scope for this thesis.

The implementation of the greedy search algorithm in this thesis is done by adding PV power production to one load bus at a time, evaluating the grid and selecting the load bus that gives the minimum or maximum of the maximum bus voltage increase, compared to the grid without any production, during the time interval of the data set. The weakest bus is selected according to

$$\Delta U_{weakest} = \max\left(\max\left|\left|U_{prod}\right| - \left|U_{noprod}\right|\right|\right) \quad \text{for all time steps and buses,} \quad (4.1)$$

and the strongest bus according to

$$\Delta U_{strongest} = \min\left(\max\left|\left|U_{prod}\right| - \left|U_{noprod}\right|\right|\right) \quad \text{for all time steps and buses,} \tag{4.2}$$

before moving on to the next set of choices. These objective functions maximise and minimise the voltage changes of all buses, respectively, to find the buses most and least affected by the PV power production.

In the second iteration, the PV power production is placed in the previously chosen bus and one additional load bus at a time, the grid is evaluated and the optimal bus according to the optimisation criterion is selected.

This continues step by step until all load buses have been selected and an order of impact is given. For Hallonvägen, this means $\sum_{n=1}^{67} n = 2278$ full calculations have to be made on the grid twice since both the weakest and strongest orders are sought. The implemented algorithm is described in Figure 4.1.

4.3 Power Factor of PV Power Systems

According to literature and research such as [20, 26], reactive power is a useful tool to control voltage in a power grid. Generation of reactive power can be used to increase the voltage at voltage drops and consumption of reactive power can be used to decrease the voltage at voltage swell.

The PV model used in this thesis only generates active power values for the PV power production. In order to evaluate whether reactive power affects the voltage and thus how much PV power production is possible in the grid, it is assumed that the power inverters used with the PV power systems can be set to a power factor other than one. An inductive power factor means that reactive power is consumed and a capacitive power factor means that reactive power is generated.

The reactive power values are calculated using

$$Q_{prod,ind} = \frac{P_{prod}}{\cos\varphi} \sin\left(\arccos\left(\cos\varphi\right)\right) = P_{prod} \tan\varphi \tag{4.3}$$

for inductive generation and

$$Q_{prod,cap} = -\frac{P_{prod}}{\cos\varphi} \sin\left(\arccos\left(\cos\varphi\right)\right) = -P_{prod} \tan\varphi \tag{4.4}$$

for capacitive generation. The combined complex power is then calculated as

$$S_{prod} = P_{prod} + jQ_{prod}. \tag{4.5}$$

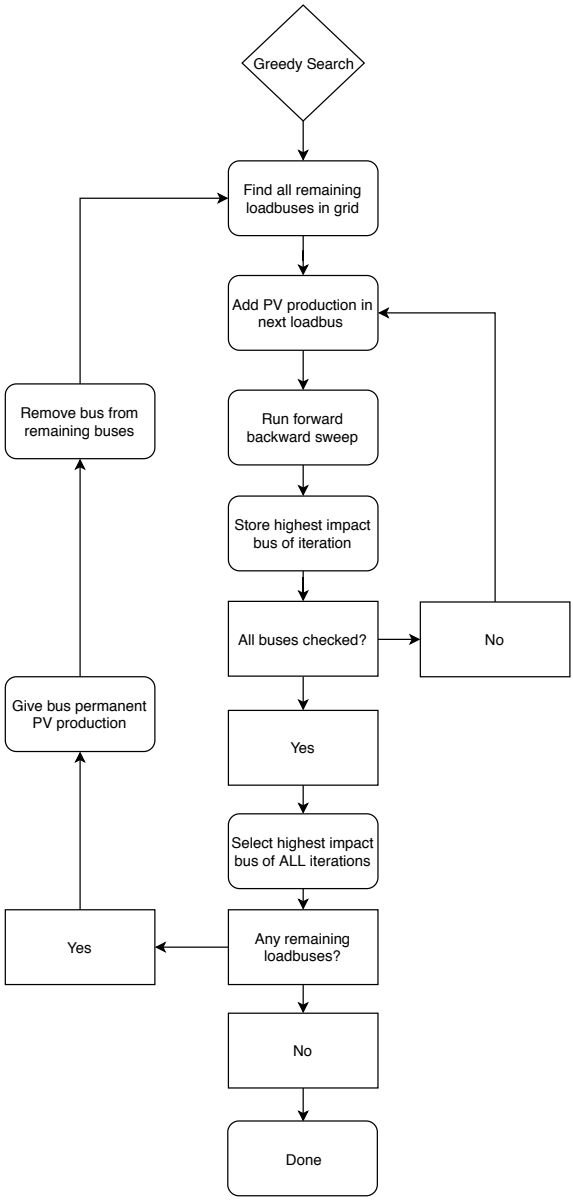

Figure 4.1: Flowchart describing the implemented greedy search algorithm.

4.4 Energy Storage Systems

The purpose of the implementation of energy storage systems, ESS:s, is to add controllable loads to the system. When the load is increased, some of the power produced by the PV power system will charge the ESS instead of being pushed onto the grid which would have increased the voltage. In this implementation, the ESS is charging when the voltage at its bus reaches a threshold of 245 V (line-to-neutral), but a smarter system using, for example, a system-level controller considering all bus voltages, could be used.

5
Results

In this section, the results from the analyses in Chapter 4 are presented. Due to many buses in the evaluated real grid, many time steps and many different PV power production cases, large amounts of data is generated. The results presented in this chapter do not cover every single data point, but instead summarises the most interesting data used to answer the questions from Section 1.1.

5.1 Normal Case Without Production

The range of voltages in all load buses at Hallonvägen with normal consumption and no production are presented in Figure 5.1. The bars show the minimum, maximum, and average voltages for each season, where winter is December to February, spring is March to May, summer is June to August and fall is September to November. The maximum voltage is approximately 242 V, is reached in the summer and corresponds to a margin of 11 V to the upper voltage limit at 253 V. The minimum voltage is slightly below 229 V, occurs in the winter and corresponds to a margin of almost 22 V to the lower voltage limit at 207 V.

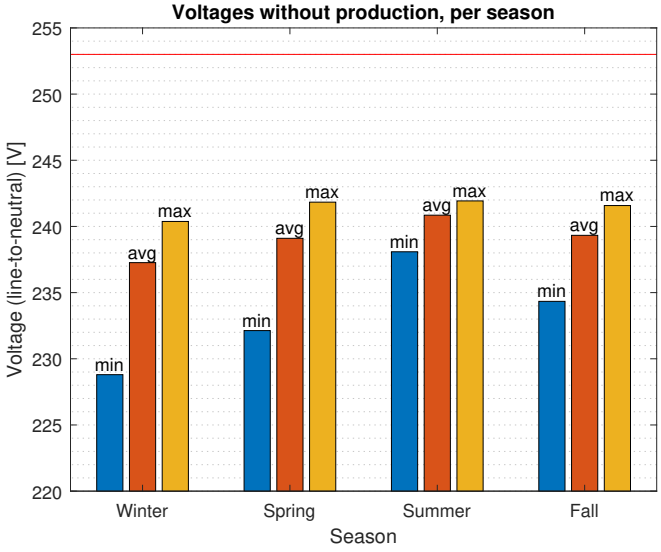

Figure 5.1: Voltages in all load buses at Hallonvägen with normal consumption and no production, with minimum, maximum and average values for each season. The red line indicates the upper voltage limit of 253 V.

In Figure 5.2, the buses with the highest and lowest mean voltages are presented. They show the full-year timeline, with the red horizontal lines representing the upper and lower voltage limits. It can be noted that the voltage difference between the two buses with the highest and lowest mean voltages is small.

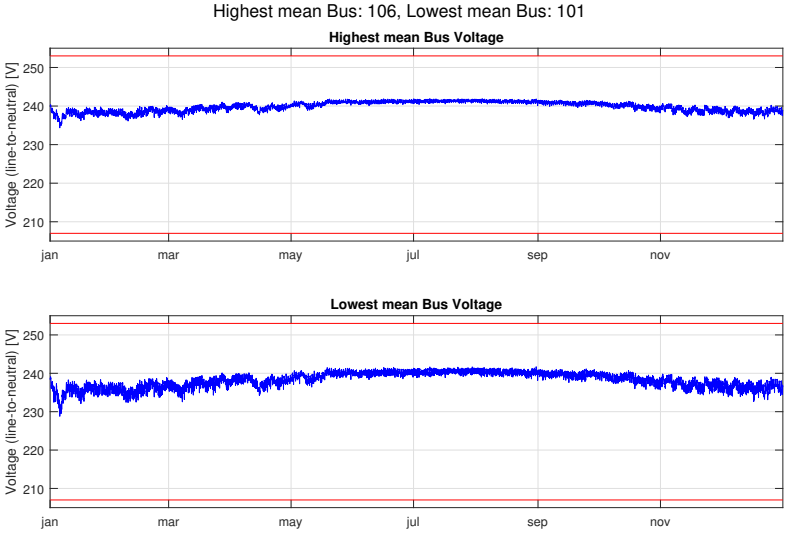

Figure 5.2: Voltages over a year for buses with the highest and lowest mean voltages in the case of no production.

5.2 PV Power Production at All Loads

For PV power production at all loads (50 % of a default PV power system, i.e. 4 kW peak), the results are presented in Figure 5.3. The maximum voltage is slightly above 250 V, is reached in the summer and corresponds to a margin of less than 3 V to the upper voltage limit at 253 V. The minimum voltage is slightly below 229 V, occurs in the winter and corresponds to a margin of almost 22 V to the lower voltage limit at 207 V.

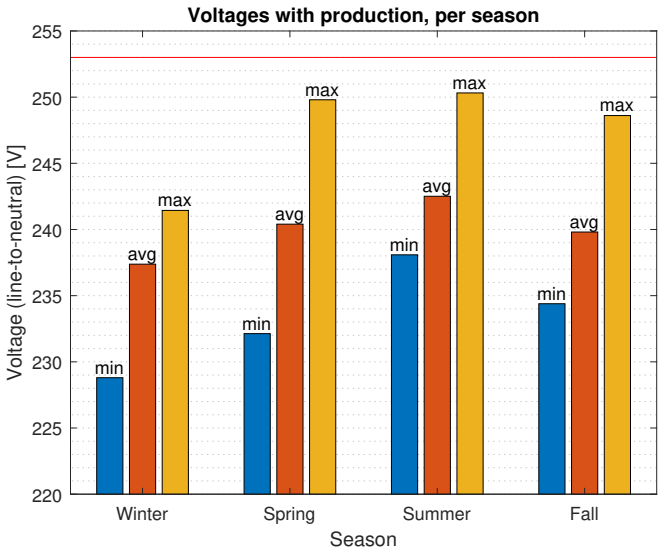

Figure 5.3: Voltages in all load buses at Hallonvägen with normal consumption and 50 % of a default PV power system at each load, with minimum, maximum and average values for each season. The red line indicates the upper voltage limit of 253 V.

In Figure 5.4 the buses with the highest and lowest mean voltages are presented. They show the full-year timeline, with the red horizontal lines representing the upper and lower voltage limits. It can be noted that the highest and lowest mean voltage buses are very similar.

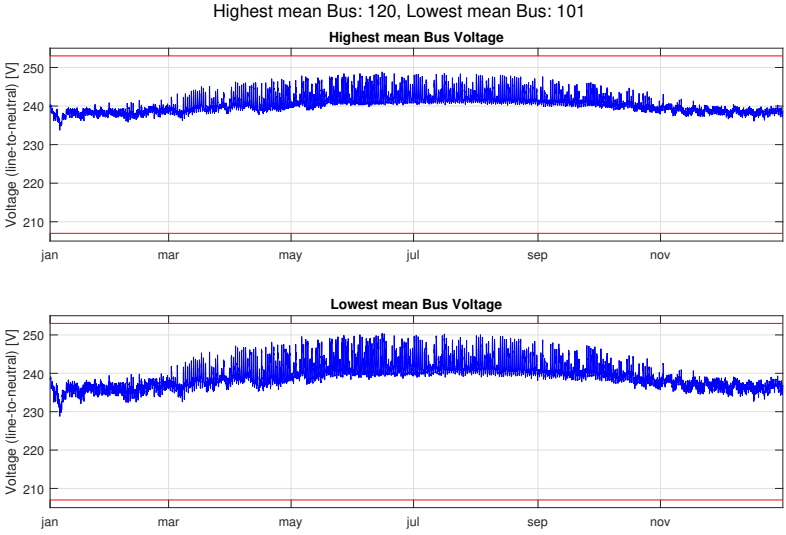

Figure 5.4: Voltages over a year for buses with the highest and lowest mean voltages in the case of 50 % of a default PV power system at each load.

5.3 Evenly Distributed PV Power Production

The results when PV power systems are distributed evenly in the real grid T085 Hallonvägen are presented herein.

Robustness of the grid is limited by the first bus that reaches the voltage limit. Since the grid contains 67 load buses and 120 buses in total, presenting each individual voltage for each bus and time step becomes quite messy and chaotic. Instead, when evaluating the grid, the margin to the voltage limit is presented as distribution curves for all bus voltages.

In Figure 5.5, the voltages of all buses are compared to the voltage limits and then plotted against the PV power production per PV power system. The dashed line at the bottom represents the value closest to the voltage limit, with negative values denoting that the limit has been exceeded. Lines labelled with a percentage value are quantiles. For example, the threshold is reached for 20 % of the time when the production is 30 kW (peak) per system. When the production is 8 kW (peak) per system, the threshold is exceeded less than 10 % of the time.

The threshold for what the grid can handle without overshooting the voltage limits is 5.15 kW (peak), approximately 64 % of the default system's peak PV power production, per household. In Figures 5.6 and 5.7, the critical bus voltage and

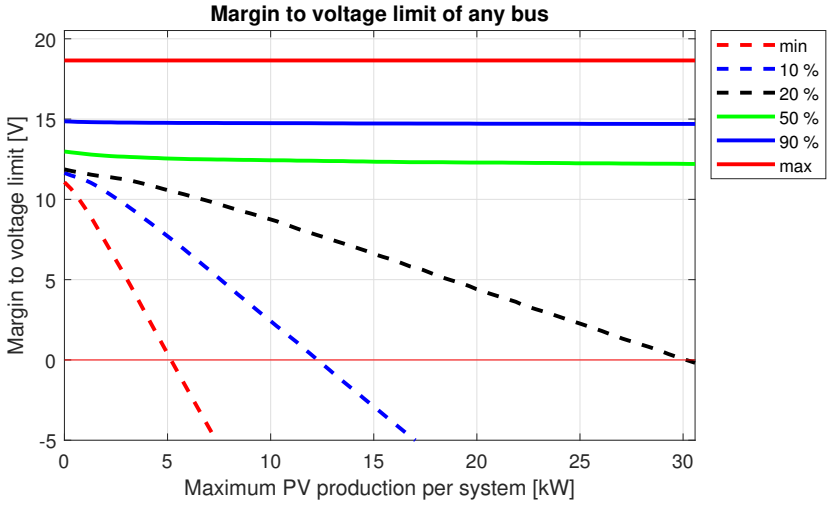

Figure 5.5: Voltage distribution as a function of production per household when PV power production is distributed evenly, during a year.

power is plotted over the year and compared to the case with no production. The critical bus is defined as the bus that first reached the voltage limit which is marked as the horizontal red line in the plots.

In Figure 5.6 the voltage and power of the critical bus, in this case bus 99 which is a load bus, is plotted when the voltage limit first was reaches in the grid. At this

point the PV power production per household is 5.15 kW (peak), which translates to a total production of 345 kW (peak) for the entire grid. The highest voltage values are found during the summer when the bus power is negative, denoting that there is more production than consumption. In Figure 5.7, the critical bus volt-

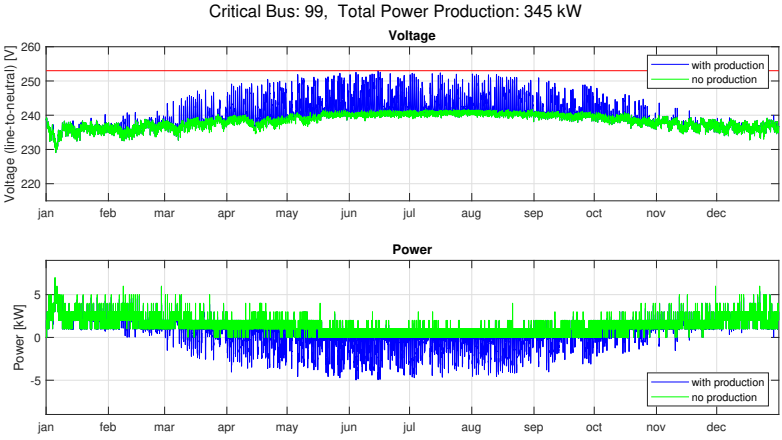

Figure 5.6: The critical bus voltage over the year when the voltage limit is reached. Bus number 99, total production in the system is 345 kW (peak).

age and power, in this case bus 99 which is a load bus, is plotted and compared to the case of no production when the PV power production is at one default PV power system, approximately 8 kW (peak) per household which equals a total production of 539 kW (peak). With production this high all across the grid, the critical bus has voltages far beyond the limit for the better part of six months. In Figure 5.8, the same bus as in Figure 5.7 is plotted, during the same production conditions, but when the transformer has had its secondary voltage lowered by 5 %. It should be noted that the voltages are below 230 V when there is no production, but the voltage limits are not reached.

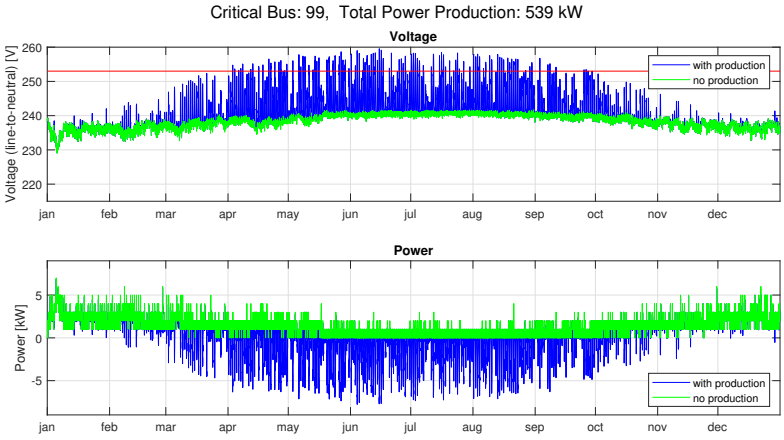

Figure 5.7: The critical bus voltage over the year when all households have PV power production. Bus number 99, total production in the system is 539 kW (peak).

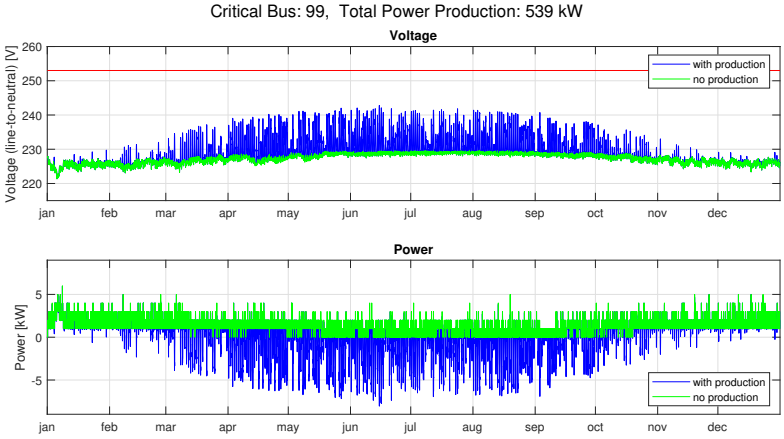

Figure 5.8: The critical bus voltage over the year when all households have PV power production but with the transformer secondary-side voltage scaled down by 5 %. Bus number 99, total production in the system is 539 kW (peak).

5.4 Selectively Distributed PV Power Production

The results when PV power systems are distributed in a certain selected order in the real grid, Hallonvägen, are presented herein. The weak and strong placement orders are defined as the results from the greedy search using the two different objective functions presented in Equations (4.1) and (4.2), respectively.

5.4.1 Weak Placement

In Figure 5.9, the voltages of all buses are compared to the voltage limits and then plotted against the number of PV power systems in the grid. The dashed line at the bottom represents the value closest to the voltage limit, with negative values denoting that the limit has been exceeded. The threshold for what the grid can handle without exceeding the voltage limit is 28 PV power systems, 42 % of all households in the grid.

In Figure 5.9, the x-axis shows the number of PV power systems instead of the size of the PV power system, which was the case when the results from the even distribution were presented. The sizing of the PV power systems in this section is kept as a default PV power system with a production of 8 kW (peak).

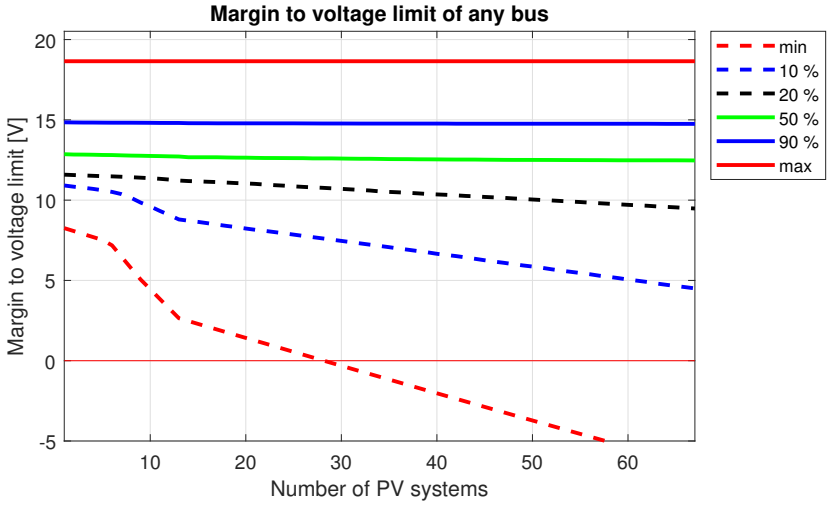

Figure 5.9: Voltage distribution as a function of the number of PV power systems in the grid when PV power production is placed in the weak order, during a year.

In Figure 5.10, the voltage and power of the critical bus, in this case bus 99 which is a load bus, is plotted when the voltage limit first was reached in the grid. At this point, the number of PV power systems in the grid is 28 (42 % of the households) which equals a total production of 225 kW (peak) for the entire grid, roughly 35 % lower than when placing the systems evenly and staying within the voltage limits. The highest voltages are fund during the summer when the bus power is negative, meaning that there is more production than consumption.

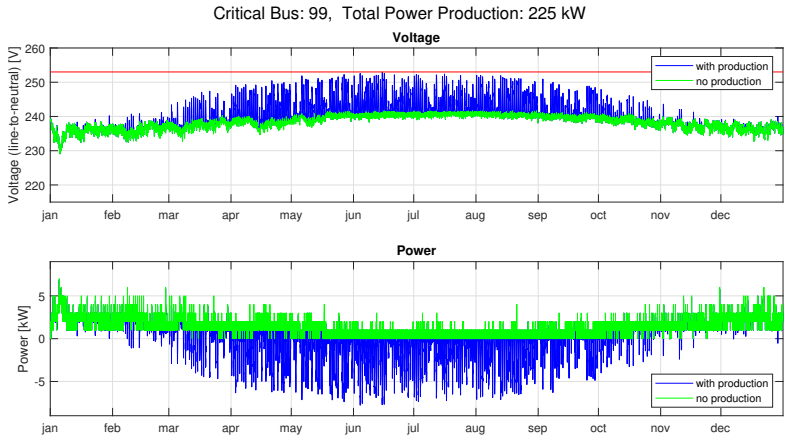

Figure 5.10: The critical bus voltage over the year when the voltage limit is reached (PV power system placed in the weak order). Total PV power production is 225 kW (peak) which equals approximately 28 households.

In Figure 5.11 the critical bus voltage and power, in this case bus 99 which is a load bus, is plotted when the total production in the grid is similar to the total production of the evenly distributed case when the voltage limit was reached (Figure 5.6). With an even distribution of PV power systems, more power can be produced than when PV power systems are placed in the weak order.

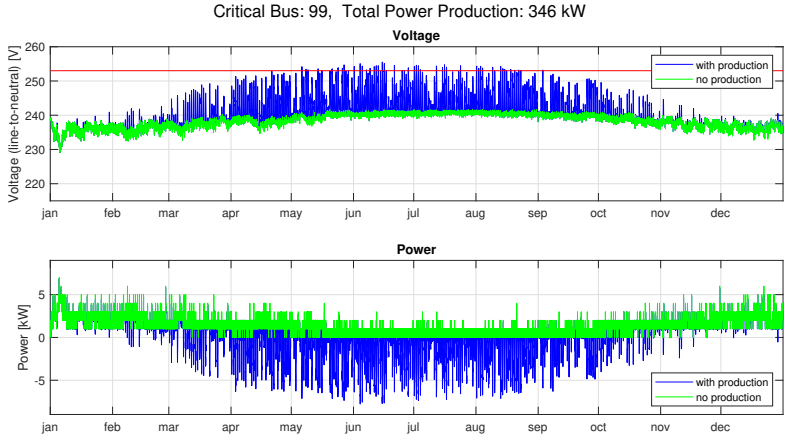

Figure 5.11: The critical bus voltage when PV power systems are placed in the weak order and total production in the grid is similar to the even distribution limit. Total PV power production is 346 kW (peak) which equals approximately 43 households.

5.4.2 Strong Placement

In Figure 5.12, the voltages of all buses are compared to the voltage limits and then plotted against the number of PV power systems in the grid. The dashed line at the bottom represents the value closest to the voltage limit, with negative values denoting that the limit has been exceeded. The threshold for what the grid can handle without exceeding the voltage limit is 49 PV power systems, approximately 73 % of the households.

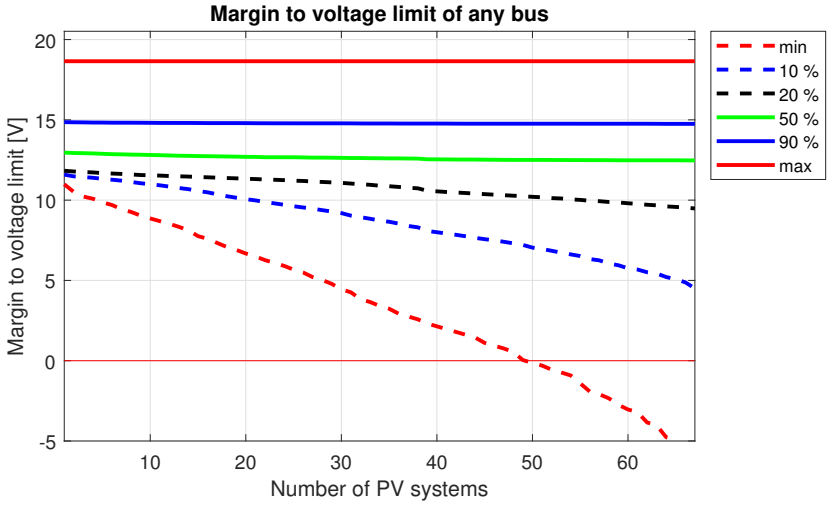

Figure 5.12: Voltage distribution as a function of the number of PV power systems in the grid when PV power production is placed in the strong order, during a year.

In Figure 5.13, the voltage and power of the critical bus, in this case bus 47 which is a load bus, is plotted when the voltage limit first was reached in the grid. At this point the number of PV power systems in the grid is 49, 73 % of the households which equals a total production of 394 kW (peak) for the entire grid. When placing the PV power systems in the strong order, the total production the grid can handle is 49 kW (peak) higher than when distributed evenly and not exceeding the voltage limit. This corresponds to an increase of approximately 14 %.

In Figure 5.14, the voltage and power of the critical bus, in this case bus 120 which is a load bus, is plotted when the total production in the grid is similar to the total production when the voltage limit was reached in the even distribution case, as shown in Figure 5.6.

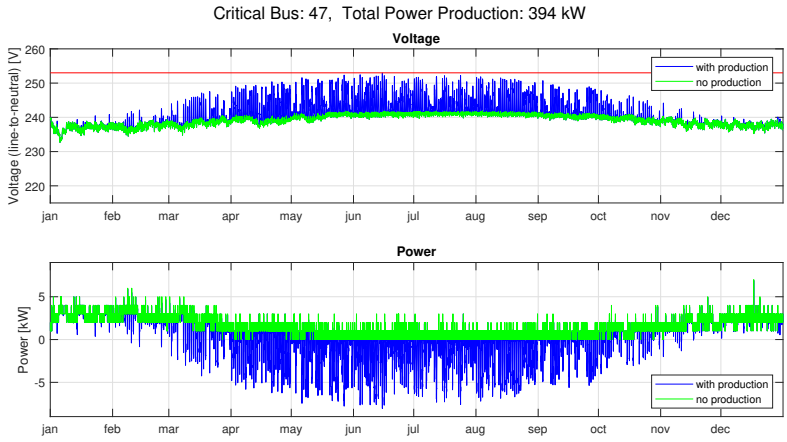

Figure 5.13: The critical bus voltage over the year when the voltage limit is reached with PV power systems placed in the strong order. Total PV power production: 394 kW (peak).

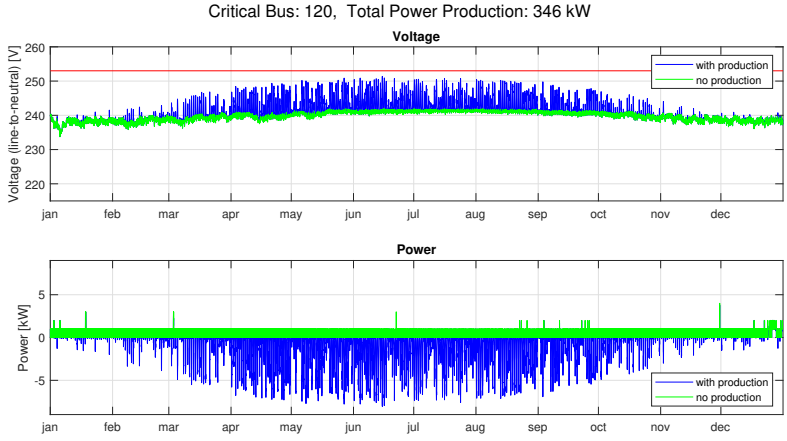

Figure 5.14: The critical bus voltage when PV power systems are placed in the strong order and total production in the grid is similar to the even distribution limit. Total PV power production: 346 kW (peak).

5.5 Power Factor of PV Power Systems

Even distribution of PV power systems is also evaluated using different power factors and presented herein. The voltages of all buses are compared to the voltage limits and then plotted against the PV power production per PV power system. The dashed line at the bottom represents the value closest to the voltage limit, with negative values denoting that the limit has been exceeded. Lines labelled with a percentage value are quantiles.

In Figure 5.15, the results for the standard case with power factor one is shown. The threshold for what the grid can handle without overshooting the voltage limits with this power factor is 5.15 kW (peak) PV power production per household.

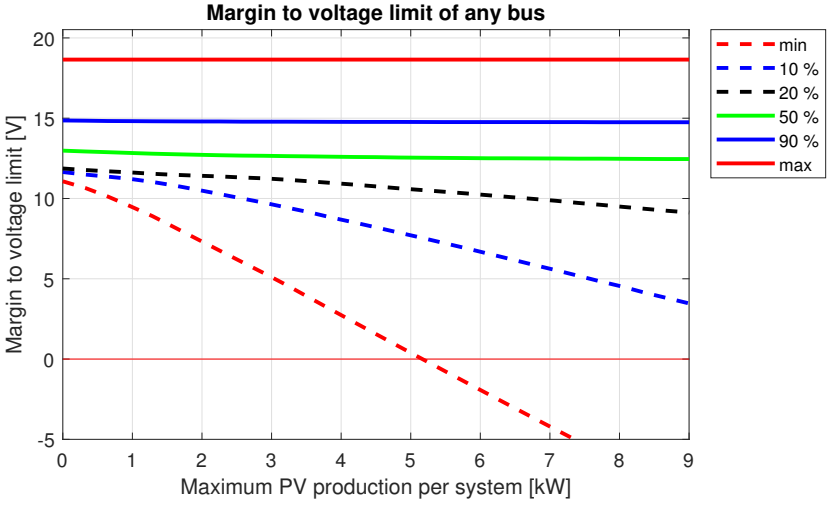

Figure 5.15: Voltage distribution as a function of production per household when PV power production is distributed evenly, during a year, with PV power factor one (only active power).

In Figure 5.16, the results for the case with power factor 0.6 capacitive is shown. The threshold for what the grid can handle without overshooting the voltage limits with this power factor is 4.50 kW (peak) PV power production per household. This is lower than the case with power factor one.

In Figure 5.17, the results for the case with power factor 0.6 inductive is shown. The threshold for what the grid can handle without overshooting the voltage limits with this power factor is 6.45 kW (peak) PV power production per household. This is higher than the case with power factor one and thus also higher than the capacitive case.

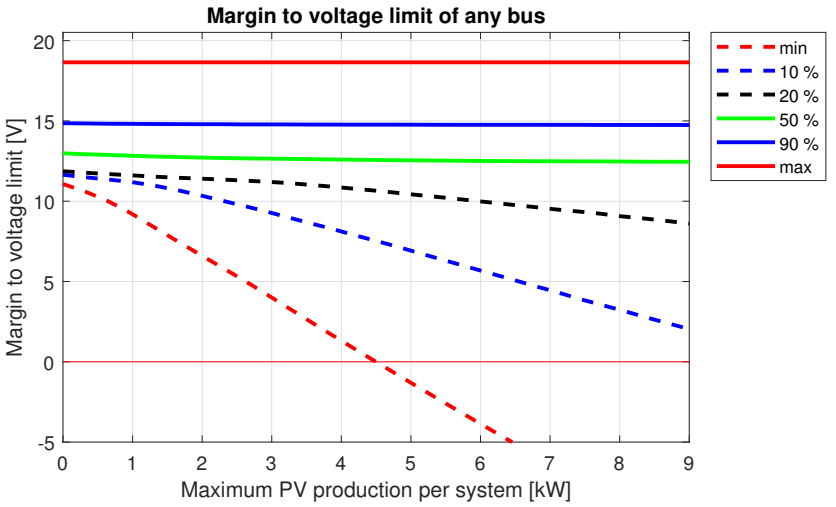

Figure 5.16: Voltage distribution as a function of production per household when PV power production is distributed evenly, during a year, with PV power factor 0.6 capacitive.

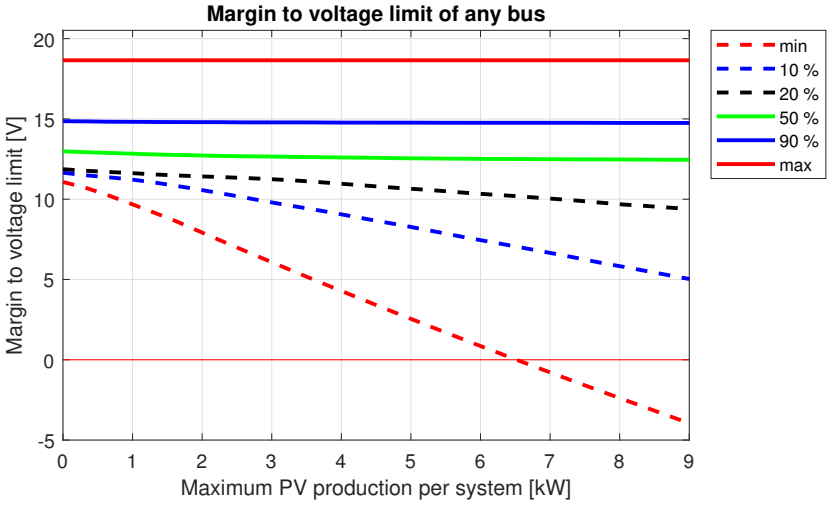

Figure 5.17: Voltage distribution as a function of production per household when PV power production is distributed evenly, during a year, with PV power factor 0.6 inductive.

5.6 Energy Storage Systems

One solution to counteract voltage swell during PV power production is to install energy storage systems. As described in Section 3.4, two variants of ESS:s are implemented. One variant has a large ESS at bus 120, a load bus close to the transformer, and one variant has one small ESS at each load bus. Their specifications are presented in Table 3.5.

In Figure 5.18, the results of energy storage system placement within the grid are presented. Without ESS, the maximum voltage is just above 250 V, within 3 V from the upper voltage limit at 253 V. With 67 small ESS:s, the maximum voltage is reduced to just below 248 V, thus now having a margin of just above 5 V to the limit. With one large ESS, the maximum voltage is approximately 249.5 V, meaning a margin of 3.5 V to the upper voltage limit. Notable here is that the minimum voltage is drastically reduced from around 238 V in the first two cases to just below 222 V here, but this is still well above the lower voltage limit at 207 V. Only the results for the summer (June to August), when the PV power production is at its highest, are presented here, since this is when the energy storage systems have the most impact.

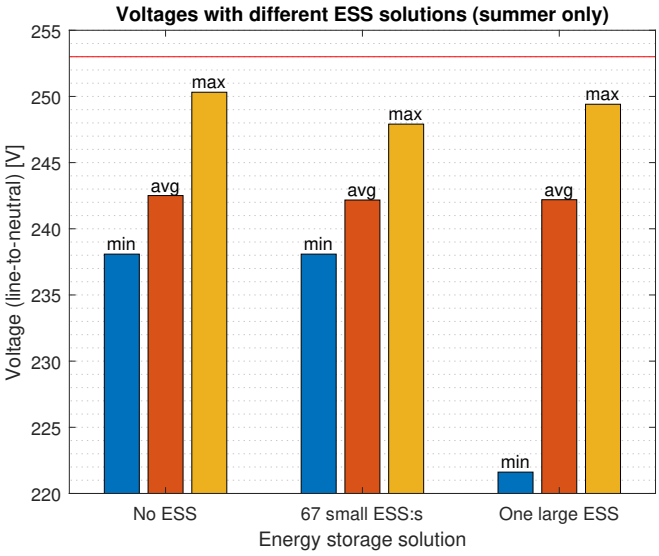

Figure 5.18: Voltages in all load buses at Hallonvägen with PV power production in all load buses and two variants of energy storage systems.

Even distribution of PV power production is tested again in the same manner as in Section 5.4, but now with energy storage systems enabled. For comparison, the case without energy storage system is presented in Figure 5.5, where the maximum PV power production per system (before exceeding any voltage limit) is 5.15 kW (peak).

In Figure 5.19, the results are presented for the version with one small energy storage system at each load bus. The maximum PV power production per system before any voltage limit is hit is approximately 6.20 kW (peak) in this case. This is notably higher than the case with no ESS.

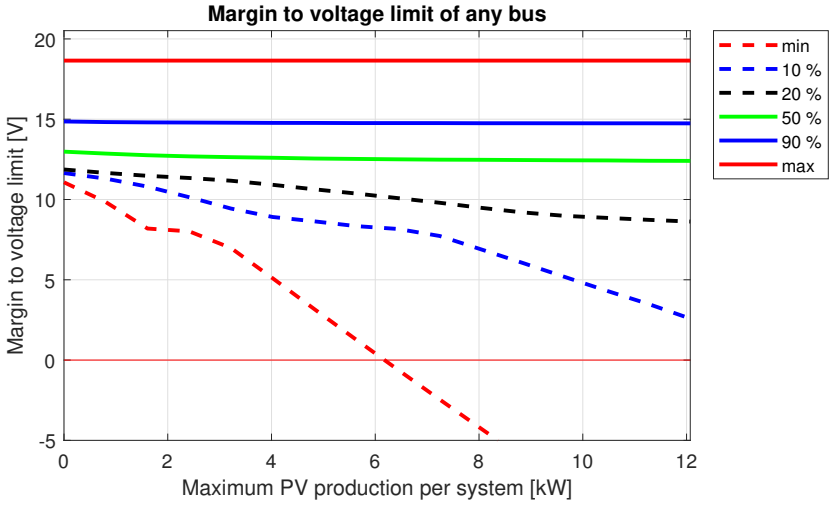

Figure 5.19: Voltage distribution as a function of production per household when PV power production is distributed evenly, during a year, with one small ESS at each load.

In Figure 5.20, the critical bus, bus 99, is shown during the same production case as when presented in Section 5.3, where it did not have an ESS. It can be seen that the voltages are still exceeding the limit but now a lot less, showing the impact of the ESS:s.

In Figure 5.21, the results are presented for the version with one large energy storage system close to the transformer. The maximum PV power production per system before any voltage limit is hit is approximately 5.63 kW (peak) in this case. This is higher than the case with no ESS, but lower than the case with one small ESS at each load.

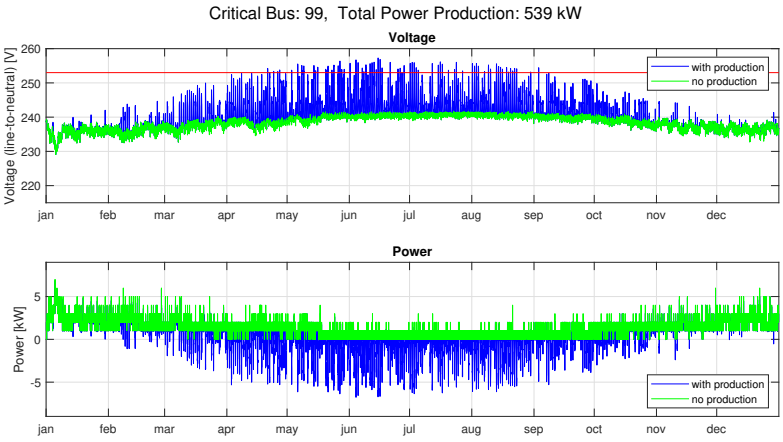

Figure 5.20: The critical bus voltage and power when PV power systems are placed evenly together with small ESS:s at each load. Default PV power systems are used (8 kW peak) and the total power production in the system is 539 kW (peak).

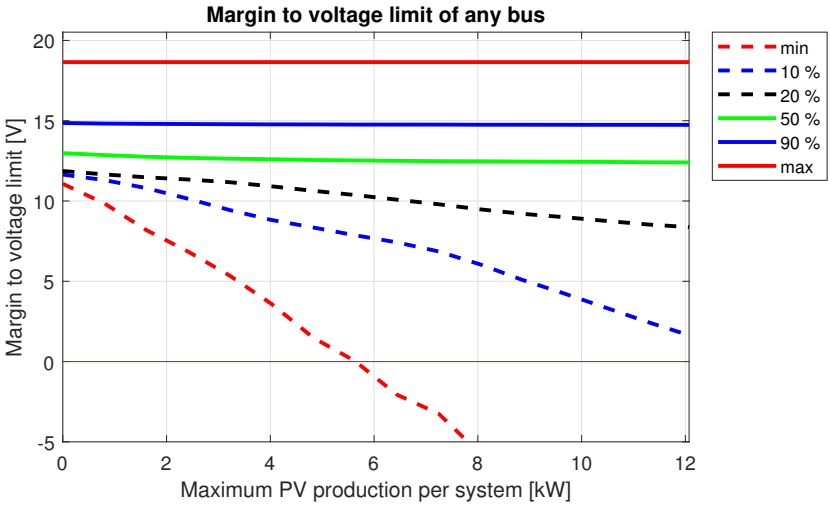

Figure 5.21: Voltage distribution as a function of production per household when PV power production is distributed evenly, during a year, with one large ESS close to the transformer.

In Figure 5.22, the critical bus is shown when a large ESS was placed at a bus close to the transformer. It can be seen that the voltages are still exceeding the limit. Not as much as when no ESS is used, but more than when small ESS:s at each load is used.

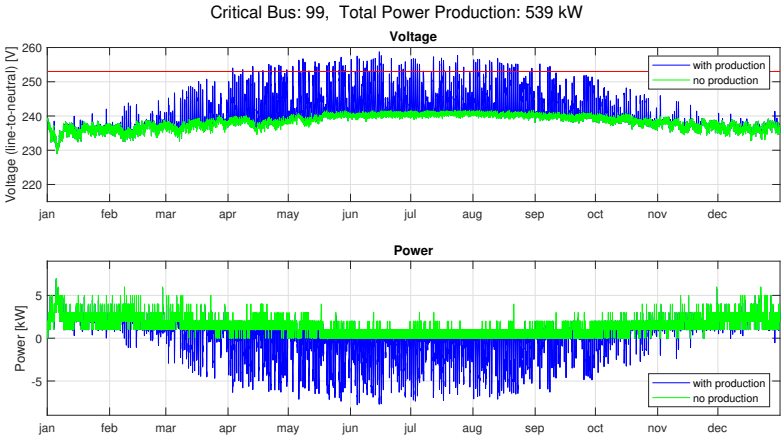

Figure 5.22: The critical bus voltage and power when PV power systems are placed evenly together with a large ESS at bus 120, a load bus close to the transformer. Default PV power systems are used (8 kW peak) and the total power production in the system is 539 kW (peak).

The amount of energy stored in the energy storage systems during the year, instead of being pushed onto the grid and thus increasing the voltage, is presented in Table 5.1 for both ESS configurations.

	Energy Stored (per system)	Energy Stored (total)
Small	554 kWh	37 108 kWh
Large	35 402 kWh	35 402 kWh

Table 5.1: The amount of energy stored in the energy storage systems during the year, instead of being pushed onto the grid and thus increasing the voltage.

6
Discussion

In this chapter, the questions in Section 1.1 are discussed using the results from Chapter 5. This includes to what extent the results are valid and how different choices and prerequisites affect the results.

For easier reading, the questions asked are repeated here. The objective of this master thesis project is to investigate the following issues:

1. How much PV power production can a distribution grid handle before the electric power quality deteriorates?
2. How does the placement of PV power systems in the grid affect the electric power quality?
3. Can electric power quality be improved by changing the power factor of the PV power systems?
4. Can electric power quality be improved by placing energy storage systems within the grid?

6.1 Modelling

In this section, the choices made when modelling the system are discussed.

6.1.1 Consumption and Production Data

Since the consumption data is stored by Tekniska verken as accumulated integer values (kWh), the load profiles shown in Figure 2.8 might not be entirely representative for the real power consumption. A value of zero before a value of one could indicate a real consumption value between 0 kWh and 0.99 kWh. This makes the consumption data quite spiky, which in turn causes spiky voltage results. This could possibly have been taken care of by filtering the data, but this is not tested since what is most interesting is the worst-case result which is given by the raw data.

The PV power production is assumed to simultaneously follow the same power profile at all load buses in the grid. In reality, this would only occur if things blocking the PV power system from the sun (such as clouds), would occur at the same time at all places, if all households had exactly the same PV power system specifications and the installations had the same orientation and tilt everywhere. That a grid would have PV power systems installed in this manner in reality is unlikely, but it is assumed to be a reasonable simplification for this thesis and will produce a worst-case result.

Because of the consumption data being stored as integers and PV power production being at a higher accuracy, the exact locations and time steps when the grid is found to fail in electric power quality might not be entirely correct. If a peak in PV power production occurs when the consumption data has a zero value stored due to the accumulated integer values, the results might not represent reality as exactly as non-accumulated values would have.

6.2 Simulation

A few aspects regarding the simulation of the system are discussed in this section.

6.2.1 Forward Backward Sweep Method

The FBSM method described in Section 3.1 is an iterative method which always uses the latest available data (estimates or results) to always try to find a better solution. If the solution changes less between two iterations than a limit set in advance, convergence is assumed. It cannot be guaranteed that convergence will occur or that the method will converge for any system. Specifically, it cannot handle grids with parallel connections or non-radial grids, at least not in the current implementation.

Since the FBSM solver calculates all connections in a grid one by one, the number of calculations and thus the calculation time increases linearly with grid size. The number of iterations needed for convergence is similar for a small and a large grid,

though, and typically between five and ten iterations. For the Hallonvägen grid and full-year hourly data, the calculation time is typically around 100 seconds on a contemporary mid-range laptop computer. This is acceptable when calculating a single test case, but causes exhaustive time consumption when running algorithms such as the greedy search requiring tenths of hours of computation time. It would also pose an issue if the implementation would be used for optimisation purposes, which, however, is not the case in this thesis. Possibly, the FBSM solver could be sped up if implemented in a low-level language such as C instead of in MATLAB.

6.2.2 Validation

There is no voltage data available from Tekniska verken for the Hallonvägen grid which could be used to verify the voltages calculated using the FBSM solver. In order to do this, it would require voltage measurements from the same period, with the same sample rate and at the same places as the power measurements.

For validation of the FBSM solver, the test system described in Section 3.2 is designed and implemented. This is a very small system with two loads, three connections and four buses, but with the advantage that it is possible to perform calculations on by hand with reasonable effort. This validation does not cover everything, but it provides some certainty that the results are correct.

The assumption of symmetricity over the three electric phases is made in order to keep the complexity of the models as well as the computation time at a reasonable level. A contributing factor is also that the household consumption data supplied by Tekniska verken does not specify the load per phase, but only the total for each household. In a real grid, the load is never perfectly symmetric but adjustments can be made to achieve better symmetricity by changing, for example, which power outlets in a household are connected to each phase. Most of the larger PV power systems are also connected to all three phases.

6.2.3 Energy Storage Systems

Due to the time constraints of the thesis work a very simple energy storage system (ESS) is implemented. The implementation only acts as an additional load on the bus it is added to. The threshold for when to activate the ESS is set to 245 V (line-to-neutral) based on previous knowledge of the grid behaviour. The sizing of the small ESS is set to be approximately the size of a small electric vehicle battery and the large ESS's size is set arbitrarily, but to be significantly greater than the small systems. Discharging of the ESS is modelled as a full discharge occurring instantly when the storage is full.

The ESS is implemented as a measure to counteract the voltage peaks, and despite its basic implementation, it seems to fill this purpose. Some of the power produced by the PV power systems is put in the ESS instead of being forced onto the grid, which would have increased the voltage.

6.3 Results

Results discussed in this section are only directly applicable to the Hallonvägen grid, since another grid would have different transformers, cables and number of loads in the grid. However, this grid is assumed to be representative for a typical residential housing area in Sweden.

6.3.1 Normal Case Without Production

In Figure 5.1 the minimum, average and maximum voltages over the seasons can be seen in the grid's original state with no PV power production. The maximum voltages over the seasons stay quite the same at around 242 V (line-to-neutral) which occurs when consumption is very low. The minimum voltages fluctuate a bit with its lowest being in the winter, likely due to the higher consumption required to heat the households. Neither the lowest nor the highest voltages are close to the limits which is to be expected since the grid has been designed for this purpose.

6.3.2 PV Power Production at All Loads

As an illustration of how the voltages change when PV power production is added, an arbitrary amount set to 50 % of a default system is added to each load in the grid. This corresponds to a power production of 4 kW (peak) per load and the results are shown in Figure 5.3. The maximum voltages are significantly higher at all seasons except during the winter, as expected. The minimum voltages stay relatively unchanged compared to the zero-production case since the minimum values are found when production is low and consumption is high. The maximum values occur when consumption is low and production is high, causing the voltages to rise and in this case closing in on the upper voltage limit during three of the seasons.

6.3.3 Evenly Distributed PV Power Production

This implementation is done because it provides information of how the grid handles a widespread distribution of PV power systems. This corresponds to a situation where all households have PV power production, a scenario that is likely in the future. In Figure 5.5 it can be seen that in order to avoid reaching any voltage limit, all of the installed PV power systems would have to be smaller than 5.15 kW (peak). This is of course not an exact value, since the data used to simulate is based on hourly measurements that will have some unknown variance. If the PV power systems produce twice as much power (at peak production), not even 10 % of the voltages exceed the limit. From Figures 5.6 and 5.7 it can be seen that the voltage values peak during the summer and it can be assumed that the voltages outside of the limit occur during this time. A possible solution to stay within the voltage limits could be to scale down the voltage at the transformer's secondary side during this period.

When the PV power systems are evenly distributed with a production of 5.15 kW (peak) and total production in the grid is 345 kW (peak), the first bus to reach any voltage limit is presented in Figure 5.6. It can be seen that for the voltage to reach the limit, the production needs to be several times higher than the consumption. In Figure 5.7, the same bus is presented but with the PV power production being at 8 kW (peak) per system. The voltages at the critical bus are, in this case, outside of the limits for the most part of April to October. Under these conditions the total power production in the grid surpasses the transformer power rating (500 kVA, presented in Table 3.4) several times during the same period.

In the evenly distributed case, it is shown in Figure 5.8 that by lowering the secondary-side voltage of the transformer, a full default PV power system could be placed at each load without exceeding any voltage limit, even in the most affected bus. This means, that to avoid deteriorating electric power quality during periods of high production, it could be possible to lower the voltage at the secondary side of the transformer.

6.3.4 Selectively Distributed PV Power Production

A more realistic placement of the PV power systems is the one where only some of the houses have a PV power system installed and the rest do not. When placing the PV power systems in the weakest order, based on the greedy search results, the grid can handle 28 systems as shown in Figure 5.9. When placing them in the strongest order it takes 49 systems for the voltage to reach the limit, as shown in Figure 5.12. Considering both of these limits, one can say that PV power production will not cause problems with the electric power quality as long as the coverage is less than approximately 42 %, but will if the coverage is 73 % or more, regardless of placement.

This means, that for the entire grid, it can be said that no problems will occur as long as the total peak production stays below 225 kW (peak), but production greater than 394 kW (peak) will cause problems with the electric power quality, regardless of placement.

In Figure 5.9, a precipitous slope can be seen between PV power system number 4 and 13. This is caused by the buses in the branch beginning in bus 91 (see Figure 2.1) being selected by the greedy search and the entire branch being filled. The reason behind this choice by the greedy search has not been investigated.

The total PV power production in the grid is approximately 35 % lower when any voltage limit is reached if the PV power systems are placed in the weakest order than when the production is spread out evenly across all loads. It can be seen that when placing the PV power systems in the strongest order, the total production of the grid can be 75 % higher compared to the weakest order. This is expected and proves that placement of the PV power systems have an impact on the electric power quality.

To further show that placement is important, the critical bus is presented (see Figure 5.11) when the weakest order is used along with a total grid production

similar to the evenly distributed limit, i.e. 345 kW (peak). The critical bus during these conditions can be seen exceeding the limit substantially. However, for the strongest order, the voltage limits are not exceeded when compared to the limits found in the evenly distributed case (see Figure 5.14).

The results are impacted by the sizing of the PV power system. Here, all systems have been a default system (8 kW peak production) to emphasise the impact caused by placement within the grid. If the sizing would be smaller, the grid would likely be able to handle more PV power systems in total.

6.3.5 Power Factor of PV Power Systems

When evaluating different power factors for the PV power production, using the even distribution of PV power systems, the results show that it certainly matters what power factor the inverter used with the PV power systems is set to. The case with power factor 0.6 capacitive is the worst (see Figure 5.16), power factor one is in the middle (see Figure 5.15) and power factor 0.6 inductive is the best (see Figure 5.17).

This is as expected, since consumption of reactive power (the inductive case) will decrease the voltage and production of reactive power (the capacitive case) will increase the voltage [20, 26]. When the voltage is decreased using an inductive power factor, it is thus possible to add more PV power production (active power) without reaching the upper voltage limit. The opposite is the case for a capacitive power factor. If the grid had had problems with too low voltage instead, a capacitive power factor could have been used to increase the voltage.

If each PV power system had an automatic control system able to adjust the power factor for the power production independently (depending on the voltage measured at the bus), the PV power systems could possibly help to stabilise the voltages in the grid at a desired level instead of putting them closer to the limits.

6.3.6 Energy Storage Systems

According to the results concerning the energy storage systems, it appears to be better to have many small ESS:s at the loads instead of having one large ESS close to the transformer. The many small systems give a lower maximum voltage and a higher minimum voltage. At least in this implementation, the single large ESS causes a fairly low minimum voltage, even though it is well above the minimum voltage limit. The low voltage might be due to a rather large impedance of the connection to the chosen bus, and a very large charging power (equal to 67 small ESS:s charging simultaneously).

Since both the many small ESS:s and the single large ESS lead to lower voltages in the grid, it indicates that they fill the purpose of being able to increase the PV power production without exceeding any voltage limit. This is shown in Figure 5.19 and Figure 5.21, where it can be seen that higher PV power production power is possible.

The total accumulated energy stored in the many small ESS:s is larger than the accumulated energy stored in the single large ESS (see Table 5.1). This indicates that the implemented control strategy for when the ESS:s should charge works better for the many small ESS:s. The large ESS is only monitoring the voltage at its own bus, and thus has to wait until the voltage gets too high at this single bus, whilst the many small ESS:s monitor the voltage at many more buses and thus react more quickly.

7
Conclusions

From the results presented in Chapter 5, it can be concluded that an increase in renewable power production in distribution grids, such as photovoltaic power systems installed at households, will affect electric power quality.

In the current state of the tested real grid (Hallonvägen), there are no problems with voltage drop or voltage swell based on the data provided. However, if enough households were to install PV power systems, there are several scenarios where this could cause voltage swell large enough to reach the upper voltage limit. Even if the PV power is assumed perfectly symmetric across all the electric phases, which depending on the sizing of the PV power system might not be the case, this thesis shows that problems could still occur.

As a countermeasure for the grid operator, it could be possible to install one or more energy storage systems or to force customers to set the inverters of their PV power systems to consume reactive power, i.e. to an inductive power factor. Another possible solution could be to simply lower the voltage of the secondary side of the transformer if voltage swell is likely to occur.

Currently when Swedish grid owners design a distribution grid, only worst-case scenarios for voltage dips during the winter are taken into account. This thesis shows that the opposite scenario might have to be taken into account in the future if more households want to install PV power systems.

7.1 Future Work

There are many ways this work could be continued and some of the thoughts by the authors are presented in the bullet list below.

- Further validating the work using more and better measurement data for power and voltage. In order to further ensure the dependability of the calculations, verifying the voltage calculations with measurement data would be favourable.
- Implementing a more sophisticated ESS model, with discharge implemented and with a more advanced control strategy for charging. Further analysis of how various energy storage systems, along with the models developed in this thesis, would affect both voltages and individual households' power consumption could be interesting, as PV power systems with integrated batteries are getting more common in for example Germany [1].
- Evaluating the grid using data with higher resolution and a model considering geographical location of each load together with a weather model supporting clouds to investigate voltage transients caused by a partly cloudy day. With the current implementation, the only thing needed for such an analysis would be high-resolution measurements and the geographical models.
- The grid model and solver developed in this thesis could be used to optimise, for example, the placement of PV power system placement or optimal control of the ESS:s. Additionally, the ESS:s could be defined as electric vehicles (EV:s) and various charging strategies of the EV batteries could be assessed, with or without the PV power systems in the grid.

Bibliography

[1] Matthias Resch et al. "Impact of operation strategies of large scale battery systems on distribution grid planning in Germany". In: *Renewable and Sustainable Energy Reviews* 74 (2017), pages 1042–1063. ISSN: 1364-0321. DOI: https://doi.org/10.1016/j.rser.2017.02.075. URL: http://www.sciencedirect.com/science/article/pii/S1364032117302976 (visited on 2019-02-28).

[2] Statistics Sweden. *80 procent av elen kommer från vattenkraft och kärnkraft*. 2018-10-05. URL: https://www.scb.se/hitta-statistik/sverige-i-siffror/miljo/energi/#0f540e57-bca3-4404-b59b-4bf65fea8ded (visited on 2019-02-28).

[3] Statistics Sweden. *Antal solcellsanläggningar och installerad effekt (MW), efter region. År 2016-2017*. 2018-10-05. URL: http://www.statistikdatabasen.scb.se/pxweb/sv/ssd/START__EN__EN0123/InstSolcellNY/?rxid=baf16472-f2f7-4884-9bb2-4ece51ef399b (visited on 2019-02-28).

[4] J. von Appen et al. "Local voltage control strategies for PV storage systems in distribution grids". In: *2014 IEEE PES General Meeting | Conference Exposition*. IEEE, 2014-07, pages 1–1. DOI: 10.1109/pesgm.2014.6939234. URL: https://ieeexplore.ieee.org/document/6733334 (visited on 2019-02-28).

[5] G. Bizjak, J. Kosmac, and P. Zunko. "Modelling of substations and overhead transmission lines for computer transient calculation". In: *[1991 Proceedings] 6th Mediterranean Electrotechnical Conference*. 1991-05. DOI: 10.1109/MELCON.1991.162107. URL: https://ieeexplore.ieee.org/document/162107 (visited on 2019-02-28).

[6] H. Ramadan, A. Ali, and C. Farkas. "Assessment of plug-in electric vehicles charging impacts on residential low voltage distribution grid in Hungary". In: *2018 6th International Istanbul Smart Grids and Cities Congress and Fair (ICSG)*. 2018-04-25, pages 105–109. DOI: 10.1109/SGCF.2018.8408952. URL: https://ieeexplore.ieee.org/document/8408952 (visited on 2019-02-28).

[7] Maximilian Kronawitter. "Household Electricity Cost Reduction: Impact of Photovoltaic and Smart Integration of Electric Vehicle and Battery Storage System". Master's thesis. Technische Universität München - Professur für Elektrische Energieversorgungsnetze, 2018-03-28.

[8] Swedish Meteorological and Hydrological Institute. *Ladda ner meteorologiska observationer*. 2019. URL: https://www.smhi.se/klimatdata/meteorologi/ladda-ner-meteorologiska-observationer (visited on 2019-03-12).

[9] Xu Jingzhou and Chen Xiao. "Forward/backward sweep method based on map structure for power flow calculation of distribution system". In: *CICED 2010 Proceedings*. 2010, pages 1–4. URL: https://ieeexplore.ieee.org/document/5735853 (visited on 2019-02-28).

[10] SEK Svensk Elstandard. *Svensk Standard SS-EN 50160. Spänningens egenskaper i elnät för allmän distribution*. Technical report. Version 4. SEK Svensk Elstandard, 2011-12-07.

[11] Wikipedia contributors. *AC power — Wikipedia, The Free Encyclopedia*. 2019. URL: https://en.wikipedia.org/w/index.php?title=AC_power&oldid=884260633 (visited on 2019-03-06).

[12] Wikipedia contributors. *Power factor — Wikipedia, The Free Encyclopedia*. 2019. URL: https://en.wikipedia.org/w/index.php?title=Power_factor&oldid=883419539 (visited on 2019-03-06).

[13] J. von Appen, A. U. Schmiegel, and M. Braun. "Impact of PV Storage Systems on Low Voltage Grids – A Study on the Influence of PV Storage Systems on the Voltage Symmetry of the Grid". eng. In: *27th European Photovoltaic Solar Energy Conference and Exhibition; 3822-3828* (2012). DOI: 10.4229/27theupvsec2012-5co.8.4. URL: https://www.eupvsec-proceedings.com/proceedings?paper=17556 (visited on 2019-03-01).

[14] Nikunj Lad and Prof. Arun Pachori. "Forward and Backward Sweep Algorithm for Distribution Power Flow Analysis and Comparison of Different Load Flow Methods". In: *International Journal for Research in Applied Science & Engineering Technology (IJRASET)* 4.XII (2016). ISSN: 2321-9653. URL: https://www.ijraset.com/fileserve.php?FID=5957 (visited on 2019-02-28).

[15] M. H. Haque. "Efficient load flow method for distribution systems with radial or mesh configuration". In: *IEE Proceedings - Generation, Transmission and Distribution* 143.1 (1996-01), pages 33–38. ISSN: 1350-2360. DOI: 10.1049/ip-gtd:19960045. URL: https://ieeexplore.ieee.org/document/488057 (visited on 2019-02-28).

[16] G. W. Chang, S. Y. Chu, and H. L. Wang. "An Improved Backward/Forward Sweep Load Flow Algorithm for Radial Distribution Systems". In: *IEEE Transactions on Power Systems* 22.2 (2007-05), pages 882–884. ISSN: 0885-8950. DOI: 10.1109/TPWRS.2007.894848. URL: https://ieeexplore.ieee.org/document/4162583 (visited on 2019-02-28).

[17] Niklas Berg and Samuel Estenlund. "Solceller i elnät. Betydande andel solcellers inverkan på lågspänningsnätet". Master's thesis. Lund University,

Faculty of Engineering, Division of Industrial Electrical Engineering and Automation, 2013-06-17. URL: http://lup.lub.lu.se/student-papers/record/3405499 (visited on 2019-02-28).

[18] Emily Storm. "Framtida distributionsnät i tätort och stadsmiljö". Master's thesis. Uppsala universitet, Teknisk- naturvetenskaplig fakultet, 2017. URL: http://urn.kb.se/resolve?urn=urn:nbn:se:uu:diva-325456 (visited on 2019-02-28).

[19] Anna-Maria Roslund. "Framtidens elnät. Förändringar i landsbygdsnät vid olika framtidsscenarier". Master's thesis. Uppsala Universitet, Teknisk- naturvetenskaplig fakultet, 2017. URL: http://urn.kb.se/resolve?urn=urn:nbn:se:uu:diva-325266 (visited on 2019-02-28).

[20] Prabha Kundur. *Power System Stability and Control*. Edited by Neal J. Balu and Mark G. Lauby. McGraw-Hill, 1994-01-22. 1200 pages. ISBN: 978-0-07-035958-1. URL: https://www.ebook.de/de/product/4031445/prabha_kundur_power_system_stability_and_control.html.

[21] Arindam Ghosh. *NPTEL Electrical Engineering - Power System Analysis*. Indian Institute of Technology, Kanpur. 2019. URL: https://nptel.ac.in/courses/Webcourse-contents/IIT-KANPUR/power-system/ui/TOC.htm (visited on 2019-02-28).

[22] Yousu Chen. *YBUS Admittance Matrix Formulation*. Technical report. Pacific Northwest National Laboratory - Energy and Environment Directorate, 2015-12-18. URL: https://www.gridpack.org/wiki/images/7/7e/Ybus.pdf (visited on 2019-02-28).

[23] Thomas Franzén and Sivert Lundgren. *Elkraftteknik*. Studentlitteratur AB, 2002. ISBN: 978-91-44-01804-1.

[24] Karim Shaarbafi. *Transformer Modelling Guide*. Technical report. Alberta Electric System Operator, 2014-07-08. URL: https://www.aeso.ca/assets/linkfiles/4040.002-Rev02-Transformer-Modelling-Guide.pdf (visited on 2019-02-28).

[25] Vattenfall. *Solcellspaket*. 2019. URL: https://www.vattenfall.se/solceller/solcellspaket/ (visited on 2019-02-28).

[26] Gerald Ibe Okwe. "Concepts of Reactive Power Control and Voltage Stability Methods in Power System Network". In: *IOSR Journal of Computer Engineering* 11 (2013-01), pages 15–25. DOI: 10.9790/0661-1121525.